Title

Systematic reconstruction of an effector-gene network reveals determinants of Salmonella cellular and tissue tropism

Journal

Cell Host & Microbe, 29(10)

ISSN

1931-3128

Authors

Chen, Didi
Burford, Wesley B
Pham, Giang
et al.

Publication Date

2021-10-01

DOI

10.1016/j.chom.2021.08.012

Peer reviewed

HHS Public Access

Author manuscript

Cell Host Microbe. Author manuscript; available in PMC 2022 October 13.

Published in final edited form as:

Cell Host Microbe. 2021 October 13; 29(10): 1531–1544.e9. doi:10.1016/j.chom.2021.08.012.

Systematic Reconstruction of an Effector Gene Network Reveals Determinants of *Salmonella* Cellular and Tissue Tropism

Didi Chen[1], **Wesley B. Burford**[1], **Giang Pham**[2], **Lishu Zhang**[1], **Laura T. Alto**[1], **James M. Ertelt**[2], **Maria G. Winter**[1], **Sebastian E. Winter**[1], **Sing Sing Way**[2], **Neal M. Alto**[1,*]

[1]Department of Microbiology, University of Texas Southwestern Medical Center, Dallas, Texas, 75390, USA

[2]Division of Infectious Diseases, Center for Inflammation and Tolerance, Cincinnati Children's Hospital Medical Center, University of Cincinnati College of Medicine, Cincinnati, Ohio, 45229, USA

Abstract

The minimal genetic requirements for microbes to survive within multi-organism communities, including host-pathogen interactions, remain poorly understood. Here, we combined targeted gene mutagenesis with phenotype-guided genetic reassembly to identify a cooperative network of SPI-2 T3SS effector genes that are sufficient for *Salmonella* Typhimurium (*S*Tm) to cause disease in a natural host organism. Five SPI-2 effector genes support pathogen survival within the host cell cytoplasm by coordinating bacterial replication with *Salmonella* Containing Vacuole (SCV) division. Unexpectedly, this minimal genetic repertoire does not support *S*Tm systemic infection of mice. *In vivo* screening revealed a second effector gene network, encoded by the *spv* operon, that expands the lifecycle of *S*Tm from growth in cells to deep tissue colonization in a murine model of Typhoid fever. Comparison between *Salmonella* infection models suggests how cooperation between effector genes drives tissue tropism in a pathogen group.

Graphical Abstract

Correspondence: Neal.Alto@UTSouthwestern.edu.

*Lead Contact

AUTHOR CONTRIBUTIONS

Conceptualization: D.C. and N.M.A.; Methodology: D.C., S.E.W., S.S.W., and N.M.A.; Investigation: D.C., W.B.B., G.P., L.Z., L.T.A., J.M.E., and M.G.W.; Writing-Original Draft: D.C. and N.M.A.; Writing-Review & Editing: D.C., S.E.W., S.S.W. and N.M.A.; Funding Acquisition, S.E.W., S.S.W., and N.M.A.

DECLARATION OF INTERESTS

The authors declare no competing interests.

INCLUSION AND DIVERSITY

We worked to ensure diversity in experimental samples through the selection of cell lines. One or more of the authors of this paper self-identifies as a member of the LGBTQ+ community. While citing references scientifically relevant for this work, we also actively worked to promote gender balance in our reference list.

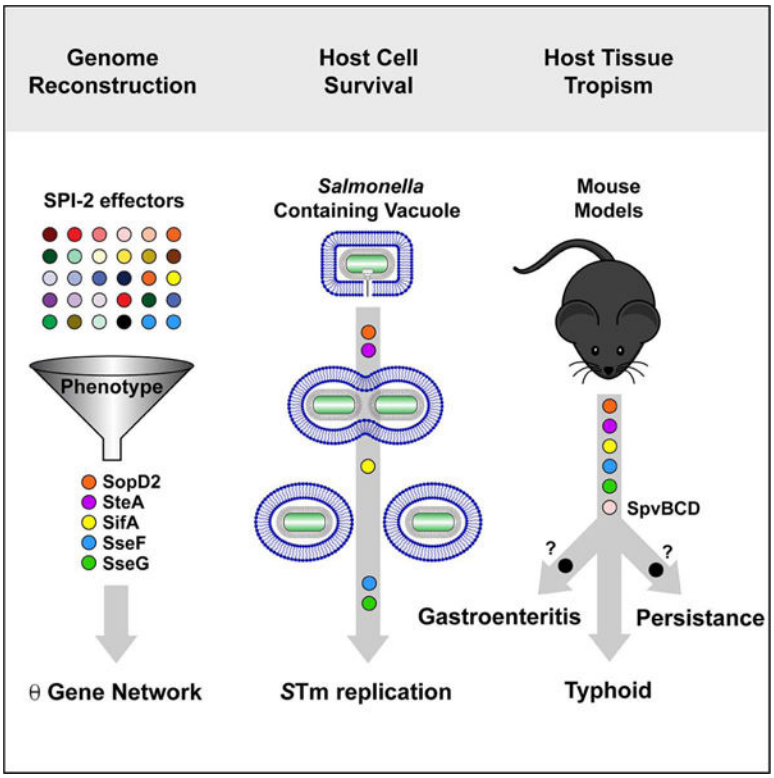

eTOC Blurb

A minimal effector gene repertoire required for *Salmonella* intracellular survival and infection of host tissues remains undefined. In this work, Chen et al. performed a systematic interrogation of the SPI-2 effector genome to identify a minimal gene network that drives cellular and tissue tropism in the *Salmonella enterica* pathogen group.

INTRODUCTION

Recent technological advances in genome synthesis have been used to successfully engineer bacteria composed of entirely essential genes (Forster & Church 2006, Gibson et al 2008, Gil et al 2004, Glass et al 2006, Hutchison et al 2016, Mushegian & Koonin 1996). This approach has revealed the fundamental genetic elements required for chromosome replication, transcription and translation, membrane biogenesis, and metabolism for bacteria grown under ideal laboratory conditions. Despite the important insights made by analyzing bacteria growth in pure culture, most microorganisms exist in microbial communities or are in direct contact with plant and animal species. Thus, more sophisticated experimental models are needed to identify the minimal genetic networks that support bacterial replication in more complex environments.

Bacterial pathogens are attractive experimental models for studying minimal gene networks required for multi-organism interactions (Cunnac et al 2011, Ruano-Gallego et al 2021, Wei et al 2015). For example, *Salmonella enterica* serovar Typhimurium (*S*Tm) encodes approximately 4500 genes (McClelland et al 2001). Despite this extensive genetic repertoire,

only a small proportion of the *S*Tm genome is solely dedicated to permitting its growth and survival within an infected host organism. The host lifecycle of *S*Tm is determined in large part by two pathogenicity islands (PIs), called SPI-1 and SPI-2, which encode independently operating Type 3 Secretion Systems (T3SS). The SPI-1 T3SS delivers a small repertoire of effector proteins into the host cell cytoplasm. These effector proteins are required for *S*Tm to invade non-phagocytic epithelial cells and to induce gut inflammation that supports bacterial colonization of the intestinal tract (Bruno et al 2009, Patel & Galan 2005). Shortly after entering the host cell, *S*Tm expresses the SPI-2 T3SS and approximately 30 effector genes (Jennings et al 2017). Translocation of these effector proteins allows intracellular *S*Tm to replicate within the *Salmonella* containing vacuole (SCV) of host intestinal epithelial cells and macrophages. Expression of SPI-2 is also required for *S*Tm to penetrate deep tissues that results in a Typhoid-like disease in susceptible animal hosts including mice (Cirillo et al 1998, Ochman et al 1996, Shea et al 1999, Shea et al 1996). Currently, a minimal effector gene repertoire that is sufficient for SCV biogenesis and pathogen infection of host tissues remains undefined. Here, we performed a systematic interrogation of the SPI-2 effector genome using both cellular and *in vivo* models of *S*Tm pathogenesis. A combination of genome minimization and phenotype guided genetic reassembly revealed five effector genes, *sopD2*, *steA*, *sseF*, *sseG*, and *sifA,* that were sufficient for *S*Tm survival in both epithelial cells and macrophages. While these genes coordinated SCV membrane division required for *S*Tm replication in the host cell, they did not support *S*Tm infection pathogenesis in a murine model of Typhoid fever. We further identified a serovar Typhimurium-specific set of effector genes encoded by the *spv* operon that extends *S*Tm's host range from mammalian cells in culture to *in vivo* infection of a natural host organism. Together, these studies provide a foundation for identifying essential genetic elements of *S*Tm intracellular growth and survival and for translating these models to more comprehensive molecular dissection of infection disease pathogenesis.

RESULTS

*S*Tm tolerates loss of function mutations in the majority of SPI-2 effector genes.

Genome sequencing revealed that the broad-host range pathogen *S*Tm SL1344 (referred here forward as *S*Tm WT) encoded full-length versions of all 30 SPI-2 effector genes (Table 1) (Jennings et al 2017). We then sought to determine which genetic loci are required for *S*Tm WT to replicate in host cells by independently deleting each effector gene (Figure 1A). A series of gene deletion guidelines were established to mitigate the potential damage caused by this large-scale mutagenesis effort. Generally, the entire coding sequence was deleted except for the first 30 nucleotides to ensure regulatory elements in the vicinity of the deleted gene were preserved. When two effector genes were closely linked, both genes were deleted using a single set of mutagenesis primers thereby minimizing genomic scarring. A special case was made for effector genes encoded by the *spv* operon (*spvBCD*) found on the *S*Tm virulence plasmid, for which mutations have been shown to have strong polar effects (Matsui et al 2001). Deletion of the *spv* transcriptional regulator *spvR* was used to eliminate expression of *spvBCD* in a single mutant strain (Guiney & Fierer 2011). In total, we generated 17 single-gene deletion mutants, 5 double-gene deletion mutants, and the

spvR deletion, compiling a library of 23 mutant strains deficient for expression of 30 SPI-2 effector genes (Table 1).

After establishing the gene deletion collection, we characterized *S*Tm growth in the H1299 human epithelial cell line (Figure 1B and 1C). H1299 cells were used as a model because they are highly permissive to *S*Tm infection at low multiplicities of infection (MOIs). A single invasive bacterial cell replicated nearly 30-fold over 18 hours (Figure 1B). In addition, *S*Tm WT replicated within the SCV, which accumulated the vacuole marker Lamp1 and migrated to the perinuclear region similar to what has been observed in other model cell types (Figure 1C, 3B, and S4C). Importantly, a Δ*ssaC* mutant, which is defective in the SPI-2 T3SS (Shea et al 1996) exhibited a severe growth defect in H1299 cells (Figure 1B and 1C). Out of the 23 mutants analyzed, deletion of only two effector gene loci, *sseFG* and *sifA*, resulted in a severe growth phenotype (Figure S1A). A Δ*sseFG* mutant failed to establish a robust replicative niche in H1299 cells whereas a Δ*sifA* mutant escaped the phagocytic vacuole and replicated to high levels in the cytosol as previously described (Figure 1B and 1C) (Beuzon et al 2002, Deiwick et al 2006). However, neither phenotype perfectly recapitulated the growth defect or morphology of the Δ*ssaC* mutant (Figure 1B, 1C and S1A).

In addition to promoting the intracellular lifecycle of *S*Tm in epithelial cells, the SPI-2 T3SS is essential for *Salmonella* survival in the murine RAW264.7 macrophage cell line (Figure 1D). Both Δ*sseFG* and Δ*sifA* exhibited severe replication defects in these cells (Figure 1D and S1B). While several other SPI-2 effector mutant strains exhibited minor growth defects in macrophage, none of these effectors were absolutely essential for intracellular *S*Tm replication (Figure S1B). We conclude that *sifA* and *sseFG* are necessary for *S*Tm infection of epithelial cells and macrophage, but the functional redundancies have masked the contribution of additional effector genes to the intracellular lifecycle of *S*Tm in these cell types.

Genome reduction: generation of a SPI-2 effectorless strain.

Next, we sequentially eliminated each of the SPI-2 effector genes from *S*Tm using Δ*spvR* as the starting strain, which was designated *S*Tm Δ1 (Table 1). Phage mediated recombination was used to delete *pipAB* from *S*Tm Δ1, resulting in the double deletion mutant *S*Tm Δ2. This process was repeated until each of the 30 effector genes were eliminated from *S*Tm as confirmed by genomic sequencing and PCR (see Methods for details). It is important to note that while each gene locus was deleted sequentially, the order was random with the exception that *sseFG* and *sifA* were the last three genes to be eliminated. This approach resulted in a SPI-2 effectorless strain, referred to as *S*Tm Efl (Table 1).

*S*Tm Efl exhibited normal growth in rich media and was capable of invading host cells, indicating that the SPI-1 T3SS dependent cellular invasion did not require SPI-2 effector genes (Figure S2A–D). However, the intracellular growth rate of *S*Tm Efl was attenuated to similar degree as the SPI-2 T3SS-deficient mutant Δ*ssaC* in both H1299 cells and RAW264.7 macrophages (Figure 1B, 1C, and 1D).

Blood borne infection of C57BL/6 mice with *S*Tm results in a lethal Typhoid-like disease. As expected, mice succumbed to *S*Tm WT infection within 5 days of intravenous (i.v.) inoculation (Figure 1E). In contrast, mice infected with *S*Tm Efl did not exhibit signs of sickness and survived for over 15 days (experimental end point) (Figure 1E). Recoverable CFUs from both the liver and spleen of *S*Tm Efl -infected mice were significantly lower than *S*Tm WT at 4 days post infection (Figure 1F). Importantly, *S*Tm Efl phenocopied the SPI-2 T3SS-deficient mutant (Δ*ssaC*) in this model (Figure 1E and 1F). Collectively, these results indicated that *S*Tm Efl lacks the essential SPI-2 effectors required for intracellular replication in host cells and for systemic infection of mice.

Mapping essential SPI-2 effector genes reveals a coordinated role for SopD2 and SteA.

In theory, there are over 1 billion possible combinations of 30 effector genes. We reasoned that the polymutant strains generated during construction of *S*Tm Efl could be used to systematically uncover essential effector genes whose activities are masked by functional redundancy. Unexpectedly, the *S*Tm Δ10 strain lacking nearly half of the total SPI-2 effector genes (see Table 1) exhibited similar intracellular growth as *S*Tm WT (Figure 2A and 2C). In contrast, *S*Tm Δ15 had a severe replication defect indicating that one or more essential effector proteins are eliminated from this strain (Figure 2A). We then analyzed *S*Tm Δ11, *S*Tm Δ12, *S*Tm Δ13, and *S*Tm Δ14 that iteratively deleted *sopD2*, *slrP*, *steA*, and *steD*, respectively (Table 1). The *S*Tm Δ11 displayed a mild replication defect, suggesting that *sopD2* deletion contributed partially to the loss of function phenotype of *S*Tm Δ15 (Figure 2B and 2C). *S*Tm Δ12 phenocopied the *S*Tm Δ11 strain, whereas the *S*Tm Δ13 strain that lacks both *sopD2* and *steA* exhibited a dramatic replication defect (Figure 2B and 2C). To determine if these effectors exhibit overlapping activities, *sopD2* and *steA* were simultaneously deleted from *S*Tm WT. The Δ*sopD2* Δ*steA* mutant exhibited a severe growth defect indicating that these genes function redundantly and contribute an essential activity to the intracellular life-cycle of *S*Tm (Figure S2E and S2F).

To determine if *sopD2* and *steA* are sufficient for *S*Tm replication in host cells, the *sopD2* and *steA* mutations were repaired in the *S*Tm Efl strain (Efl *sopD2*$^{+}$*steA*$^{+}$). Surprisingly, the total number of *S*Tm Efl *sopD2*$^{+}$*steA*$^{+}$ CFUs recovered from H1299 cells was similar to those recovered from *S*Tm WT infected cells (Figure 2D). However, *S*Tm Efl *sopD2*$^{+}$*steA*$^{+}$ bacteria escaped the phagocytic vacuole and replicated to very high levels in approximately 40% of host cells (Figure 2E and S4A). One explanation for this result is that SopD2 and SteA promote bacterial replication within the SCV, and that without cooperation with additional effector proteins required for vacuole maintenance the *S*Tm Efl *sopD2*$^{+}$*steA*$^{+}$ strain ruptures the SCV membrane and grows to high levels in the cytosol. Consistent with this interpretation, repairing the *sopD2* and *steA* loci in the *S*Tm polymutant strain that carries eleven additional effector genes (*S*Tm Δ13 *sopD2*$^{+}$*steA*$^{+}$) reestablished normal intracellular growth and SCV biogenesis (Figure 2D and 2F).

Identification of a minimal genetic repertoire supporting *S*Tm replication in host cells.

As described above, single deletion mutants of *sseFG* and *sifA* exhibited replication defects in epithelial cells and macrophages. In addition, we found that *steA* and *sopD2* cooperate with one or more of the eleven effector genes expressed by the Δ13 strain, which includes

both *sseFG* and *sifA*. We then asked if expression of these five effector genes are sufficient for *S*Tm replication in epithelial cells by restoring *sopD2*, *steA*, *sseFG*, and *sifA* in the *S*Tm Efl strain (*S*Tm Efl *sopD2*$^{+}$*steA*$^{+}$*sseFG*$^{+}$*sifA*$^{+}$). We designated this five gene combination with the Greek letter Theta (θ) (Table 1).

The intracellular replication rate of *S*Tm θ was comparable to *S*Tm WT in cell lines derived from diverse epithelial lineages and in RAW264.7 macrophage (Figure 3A and S4B). Unlike *S*Tm Efl, which failed to establish a growth niche within the SCV membrane compartment (Figure 3C), *S*Tm θ replicated to high numbers and localized to the perinuclear region of the cell at 18 hours post infection (Figure 3D). These bacteria were decorated with the SCV marker protein Lamp1 in both H1299 and Hela cells (Figure 3D and S4C). Previous studies have shown that replication of bacteria within the SCV is coordinated with SCV membrane division as each individual bacterial daughter cell is encapsulated by an autonomous membrane structure (Buchmeier & Heffron 1991, Hensel et al 1998). Similarly, both *S*Tm WT and *S*Tm θ cells were found within an autonomous SCV as visualized by Transmission Electron Microscopy (TEM) (Figure 3B and 3D). Importantly, both the intracellular growth rate and SCV morphology of *S*Tm θ was indistinguishable from the *S*Tm WT reference strain under these conditions (Figure 3A, 3B and 3D).

A co-infection trans-complementation assay was developed to determine if cytosolic delivery of the θ effector proteins were sufficient to promote bacterial replication within the SCV compartment of host cells (Figure S3). The *S*Tm Efl strain, which is unable to replicate in host cells, was co-infected with *S*Tm θ strain that translocated five SPI-2 effector proteins into the host cytoplasm (Figure S3A). Remarkably, *S*Tm θ infection promoted *S*Tm Efl replication within the SCV of co-infected cells (Figure S3A). As an extension of this study, we found that secretion of individual θ effector proteins translocated from the *S*Tm Efl strain could trans-complement the growth defects associated with the corresponding *S*Tm θ strain that lacked secretion of that effector protein (Figure S3B–D). These data confirm that secretion of all five θ effector proteins are necessary and together sufficient to support *S*Tm replication in host cells.

The θ gene effector network coordinates bacterial replication with SCV division.

As noted above, previous studies have suggested that *S*Tm replication within the SCV occurs in conjunction with SCV membrane division, resulting in both mother and daughter bacteria enclosed within an autonomous vacuole structure (Buchmeier & Heffron 1991, Eswarappa et al 2010). We then sought to determine the role of θ effector genes in this process by comparing the intracellular replication and SCV morphology of *S*Tm Efl strains expressing *sopD2* and *steA*, *sseFG*, or *sifA* either independently, or in various combinations (Figure 4A). Each of the engineered strains exhibited a growth phenotype as compared to *S*Tm WT and *S*Tm θ in both H1299 and RAW264.7 cells (Figure 4B and S4B). Interestingly however, some engineered strains executed normal SCV membrane division whereas others did not. For example, *S*Tm Efl strain expressing *sopD2*, *steA*, and *sifA* resided in an autonomous vacuole similar to *S*Tm WT (Figure 4C, Category A). In contrast, *S*Tm Efl expressing *sseFG* and *sifA* was enclosed in an SCV that encompassed multiple bacteria (Figure 4C, Category B). In addition, several *S*Tm strains were unable to maintain SCV

membrane integrity and escaped into the cytosol (Figure 4C, Category C). A synopsis of the bacterial growth phenotypes and SCV morphologies is shown in Figure 4A.

Using the assays described above, we found that SopD2 and SteA are the first SPI-2 effector proteins to modify the SCV. In support of this conclusion, expression of *sopD2* and *steA* in the absence of other effector genes (*S*Tm Efl *sopD2*$^+$*steA*$^+$) induced *S*Tm to escape the vacuole and replicate in the cytosol (Figure 4A Category C, S4A and S4C). It has been previously thought that this phenotype is due to loss of *sifA* function (Beuzon et al 2000). However, the structural integrity of the SCV was maintained in cells infected by *S*Tm Efl that lacks *sifA* (Figure 3C). Thus, delivery of SopD2 and SteA appears to initiate vacuole membrane division and in the absence of other effector proteins needed to complete the membrane division cycle *S*Tm escapes into the cytosol. Importantly, neither delivery of SseFG nor SifA alone induced bacterial escape from the SCV suggesting that these proteins function downstream of SopD2 and SteA (Figure 4A Category B, S4A and S4C).

Next, we found that SifA is the key effector protein used by *S*Tm to complete SCV membrane division initiated by SopD2 and SteA. Unlike *S*Tm Efl *sopD2*$^+$ *steA*$^+$ that failed to execute proper SCV division, expression of SopD2, SteA, and SifA together resulted in individual bacteria encompassed in a single SCV similar to that observed during *S*Tm WT infection (Figure 4A Category A, S4A and S4C). This phenotype was in stark contrast to *S*Tm Efl secreting SopD2 and SteA with SseFG (*S*Tm Efl *sopD2*$^+$ *steA*$^+$ *sseFG*$^+$), which ruptured the vacuole similar to the strain secreting SopD2 and SteA alone (Figure 4A, S4A and S4B). These data support the cooperative function of SopD2, SteA, and SifA. This finding was confirmed by the co-infection trans-complementation assay. While neither *S*Tm Efl *sopD2*$^+$*steA*$^+$ nor *S*Tm Efl *sifA*$^+$ strains functionally mimicked *S*Tm WT SCV biogenesis (Figure 4D and 4E), these strains executed proper SCV division when co-infected together (Figure 4F). Thus, these three effector proteins together initiate vacuole remodeling and execute symmetric membrane division resulting in a single bacterium per SCV.

It is important to point out that while SCV membrane division proceeded normally, the *S*Tm Efl *sopD2*$^+$ *steA*$^+$ *sifA*$^+$ strain did not replicate to high levels in the host cell (Figure 4B, S4A and S4C). Rather, combinatorial expression of these three genes and *sseFG* (note that this is the *S*Tm θ strain) was required to accelerate the bacterial replication/SCV division cycle, resulting in high levels of bacteria within the host cell (Figure 3D, 4A–B, S4A and S4C). Together, these data define a processive order of θ-gene network operation required for *Salmonella* replication within the host vacuole (see Figure 6E).

The θ gene network is not sufficient for murine pathogenesis.

Comparative evolutionary analysis of SPI-2 indicates that the θ genes are highly conserved across the *Salmonella enterica* species including host-adapted pathovars that have undergone significant genomic reduction (Jennings et al 2017). Our findings therefore suggest that SCV biogenesis is the primary driving force for purifying selection of θ effector genes across the *Salmonella* species. However, it remains unclear if the θ gene network, and by extension SCV biogenesis, is sufficient for *S*Tm to colonize and cause disease in a natural host organism. Unlike the *S*Tm WT strain, we found that i.v. delivery of *S*Tm θ failed to induce a lethal infection of mice and was nearly eliminated from the liver and spleen at

15 days post infection (Figure S5A and S5B). Thus, the θ gene effector network is not sufficient for *Salmonella* pathogenesis.

The *spv* operon is necessary, but not sufficient for systemic *S*Tm infection.

An attractive interpretation of these data is that the θ gene network is required for bacterial growth in cells, whereas additional effectors have evolved to expand the lifecycle of *S*Tm to more complex environments. To identify a genetic network that cooperates with the θ genes, we re-examined the viability of *S*Tm polymutant strains in the i.v. model of murine systemic infection. Mice infected with *S*Tm Δ5, *S*Tm Δ10, and *S*Tm Δ15 exhibited no outward signs of disease and survived for 15 days, indicating that one or more effector genes deleted in *S*Tm Δ5 (*spvR*, *pipAB*, *pipB2*, *gtgA*, and *sifB*) contribute significantly to pathogenesis (Figure S5C). Mutation in *spvR* caused a severe growth defect whereas loss of the other four effector gene loci had little effect on *S*Tm systemic infection (Figure S5D). The Δ*spvR* mutant also failed to induce lethal Typhoid-like disease (Figure S5E), which is consistent with previous reports (Yoon et al 2009). We noted however that despite the requirement of *spvR* in murine pathogenesis, the *S*Tm Efl strain expressing *spvR* alone (*S*Tm Efl *spvR*$^{+}$) was unable to cause lethal infection (Figure S5E). Thus, the effector genes expressed from the *spv* operon are necessary, but not sufficient to support systemic *Salmonella* infection.

*S*Tm Ω: a minimal effector gene network that causes Typhoid-like disease.

To determine if θ genes required for coordinating *S*Tm replication with the host SCV cooperates with effector genes encoded by the *spv* operon, we introduced *spvR* into the *S*Tm θ strain background by phage-mediated recombination (Table 1). This strain was named *S*Tm Omega (*S*Tm Ω (Table 1). Intragastric (i.g.) intubation was used to infect C57BL/6 mice with *S*Tm Ω as this model closely recapitulates the food-borne route of *Salmonella* infection (Jones & Falkow 1996, Vazquez-Torres et al 1999). As expected, we were unable to recover CFUs from the spleen or liver of mice infected with either a Δ*ssaC* mutant or *S*Tm Efl 4 days post infection, indicating that the SPI-2 T3SS and its effectors are essential for *S*Tm transmission from the gut to systemic sites (Figure 5A). In addition, *S*Tm θ, which replicated normally in tissue culture cells, failed to colonize the spleen or liver. Remarkably however, *S*Tm Ω crossed the mucosal barrier and successfully colonized deep tissues to a comparable level as *S*Tm WT (Figure 5A). The spleens of mice infected with *S*Tm Ω and *S*Tm WT exhibited comparable numbers of inflammatory monocytes, dendritic cells, neutrophils, and B-cells, indicating that the host immune system responds equivalently to these pathogen variants (Figure 5B). Consistent with this result, *S*Tm WT and *S*Tm Ω replicated at similar rates when co-infected, whereas *S*Tm WT outcompeted both the *S*Tm Efl and *S*Tm θ strain in this assay (Figure 5C). Lastly, *S*Tm Ω infected mice showed a nearly identical survival curve as those infected with *S*Tm WT (Figure 5D). In contrast, mice infected with strains deficient in the SPI-2 T3SS or SPI-2 effector genes (*S*Tm Δ*ssaC* and *S*Tm Efl, respectively) survived to the experimental end point of 15 days (Figure 5D). Thus, *S*Tm Ω functionally recapitulates *S*Tm WT infection of conventionally raised C57BL/6 mice.

Cooperation between the θ gene network and *spv* operon supports STm pathogenesis.

The *spv* operon is composed of four genes (*spvA-D*), three of which encode translocated effector proteins (*spvBCD*). Each gene was deleted from the *spv* operon of the *S*Tm Ω strain. As expected, deletion of *spvA* had little effect on *S*Tm Ω colonization of the liver and spleen (Figure 5E). In contrast, *S*Tm Ω virulence was reduced by deletion of *spvB*, *spvC*, or *spvD* (Figure 5E). While the Δ*spvB* mutant was the most attenuated, complementation of *spvB* from an alternative locus (*phoN*) only partially rescued the loss of function phenotype. These data are consistent with previous studies showing that mutation in *spvB* compromises the expression of other *spv* encoded effector genes (Matsui et al 2001). We then sought to determine whether effector genes encoded by the *spv* operon function together with the θ genes to overcome restrictions imposed by cells and tissues of the host organism. Indeed, *S*Tm Efl *sseFG*$^{+}$ *sifA*$^{+}$ *spvR*$^{+}$, which eliminates the critical effector genes *sopD2* and *steA* required for SCV biogenesis but express *spvB-D*, was avirulent in orally infected mice (Figure 5F). We conclude from these studies that cooperation between θ genes and the *spv* operon enables transmission of intracellular *Salmonella* from the mucosal barrier to systemic sites in a genetically susceptible mouse model.

The role of a minimal gene network in STm adaptation to diverse host niches.

It should be noted that our studies, so far, have been limited to cellular models and disease associated with a single strain of mice. It is therefore unclear if the θ gene network and *spv* operon are also sufficient for *S*Tm to overcome acute and chronic immunological challenges presented by alternative animal models.

Previous studies have shown that acute alteration of the gut microbiota composition with the antibiotic Streptomycin (Strep) can induce low levels of mucosal inflammation that alters the pathophysiology of *S*Tm (Barthel et al 2003). Importantly, transcytosis of *S*Tm from the gut to lamina propria in dysbiotic mice requires the SPI-2 T3SS, yet the role that individual effectors play in this process is unclear (Muller et al 2012). Consistent with previous results, Strep-treated C57BL/6 mice succumbed to *S*Tm WT infection 4–7 days post infection (Figure 6A). We observed robust caecal colonization and bacterial transmission to systemic tissues just prior to the onset of morbidity (Figure 6B). Unexpectedly, *S*Tm Ω did not cause any symptoms of disease and failed to mount a lethal infection in Strep-treated mice (Figure 6A). The burden of *S*Tm Ω in the caecum and systemic tissues was also significantly lower than *S*Tm WT at 4 days post infection. *S*Tm θ , which replicates in host cells but fails to induce lethal Typhoid like disease in untreated C57B/6 mice, exhibited the lowest burden of tissue colonization at this time point (Figure 6B). However, by 15 days of infection, both *S*Tm Ω and *S*Tm θ established nearly equivalent levels of caecal colonization and systemic burden, suggesting that these pathogen variants are readily cleared by the host immune system (Figure 6C). These data indicate that *S*Tm requires effector genes besides those of the θ-gene network and *spv* operon to efficiently colonize the host in a mouse model of *S*Tm-induced colitis.

Next, we examined chronic *S*Tm infection of the resistant mouse strain 129X1/SvJ. The *Nramp1* gene expressed in 129X1/SvJ mice prevents acute Salmonellosis, but *S*Tm can survive for long periods of time similar to chronic and persistent carrier states observed

in humans (Monack et al 2004). *S*Tm WT persisted for over 21 days in the spleen and liver of 129X1/SvJ mice without any outward sign of disease. We also detected *S*Tm Ω in these tissues after 21 days of infection (Figure 6D). However, the recovered CFUs of *S*Tm Ω were significantly lower than *S*Tm WT. These results were confirmed in C57BL/6 mice expressing a functional *Nramp1*^{G169} allele (Figure S6) (Arpaia et al 2011). It should be noted that *S*Tm θ was not recovered from the majority of infected 129X1/SvJ mice indicating that the *spv* operon plays a role in persistence (Figure 6D). Thus, the *spv* operon contributes partially to the persistence of *S*Tm Ω in genetically resistant mice, but additional SPI-2 effectors are necessary for the high levels of tissue colonization observed in *S*Tm WT infection. These data support the notion that distinct combinations of bacterial effector genes are required for *Salmonella* to occupy the variety of niches found in nature (Figure 6E). Importantly, the strain resources outlined here can provide a starting point for determining how the expansion of a minimal effector gene network can broaden tissue and host tropism of the *Salmonella enterica* species.

DISCUSSION

Here, we used a combination of genetic approaches to successfully eliminate 30 SPI-2 T3SS effector genes and then rebuild *de novo* a minimal genetic repertoire that supports *S*Tm pathogenesis in a natural host organism. Remarkably, secretion of just 5 effector proteins, SopD2, SteA, SseF, SseG, and SifA, provides *S*Tm θ strain the arsenal of weapons to support intravacuolar replication and to prevent bacterial clearance by phagocytic macrophages. Surprisingly however, the *S*Tm θ strain was unable to infect mice, which is consistent with previous studies showing that *Salmonella* survival in macrophage is necessary, but not sufficient for mouse virulence (Yoon et al 2009). We identified the *spv* operon as an independent genetic network that, when expressed in combination with θ genes, supports *S*Tm pathogenesis in a mouse model of Typhoid fever. Thus, we have defined a minimal genetic repertoire for *S*Tm replication in a cellular context and in a host organism.

The θ gene network: coordination of bacterial and host vacuole replication.

Previous studies have revealed a small repertoire of SPI-1 T3SS effector genes that are necessary and sufficient for *S*Tm to invade host cells (Zhang et al 2018). In addition, combinatorial deletions of SPI-2 effector genes have been used to uncover mechanisms of gene redundancy (Knuff-Janzen et al 2020, Matsuda et al 2019). Prior to our work however, the minimal genetic requirements for *Salmonella* to replicate within the vacuole of host epithelial cells and macrophage was unclear. TEM imaging revealed that the majority, if not all, *S*Tm clones are contained within an autonomous vacuole membrane structure at times in which the pathogen has undergone numerous rounds of replication. These findings indicate that bacterial replication must occur in unison with SCV membrane fission, as previously noted (Holden 2002). However, there is little information about the molecular mechanisms that orchestrate these events.

Our reductionist approach now indicates SopD2 and SteA cooperate directly with SifA to induce SCV membrane division. Mutagenesis studies suggest that SopD2 and SteA are the

first effector proteins to function in SCV fission (Figure 4A). Since SopD2 modulates Rab GTPases involved in endo-lysosome trafficking (D'Costa et al 2015, Spano et al 2016), these early events may include protecting the nascent SCV membrane from fusing with either lysosomes or autophagosomes that would compromise bacterial growth within the protective vacuole niche. Unlike SopD2 however, the role of SteA in SCV biogenesis is poorly understood. Its ability to bind membrane phospholipids suggests that it could localize to organelles associated with SCV fission (Domingues et al 2014, Weigele et al 2017). In addition, the precise function of SifA in SCV biogenesis remains to be determined despite this molecule being studied for over 25 years. SifA is thought to suppress lysosome functions by recruiting the host protein SKIP and Rab9 to the SCV membrane (Boucrot et al 2005, McGourty et al 2012, Ohlson et al 2008). It is unclear however if and how these interactions would induce SCV division as neither SKIP nor Rab9 have been implicated in membrane fission events. Thus, our reductionist approach has revealed insights into effector protein mechanisms, which open up new avenues of investigation into this critical event in the *S*Tm life cycle.

Although *sopD2*, *steA*, and *sifA* are the minimal genetic requirements for SCV membrane division, expression of these effector genes alone did not enable rapid *S*Tm replication similar to what is observed with the WT strain (Figure 4A). Because *S*Tm θ phenocopied *S*Tm WT, we can conclude that *sseF* and *sseG* are essential for bacterial replication during the SCV membrane division cycle. Once the SCV is established as an independent organelle, SseF and SseG stimulate transport of the SCV along microtubules to the perinuclear region of the cell (Salcedo & Holden 2003, Yu et al 2016). Because this region of the host cell is densely populated with membrane vesicles, it is plausible that this location helps stimulate fusion between the SCV and host vesicles that supply *S*Tm essential factors (e.g. nutrients) required for pathogen replication within the enclosed vacuole.

The Ω effector gene network: Licensing *S*Tm intracellular growth for *in vivo* pathogenesis.

An important finding from our approach was that *S*Tm θ failed to colonize and cause disease in orally infected mice. These data are consistent with reports showing that intracellular replication, while critical to infection, is not sufficient for *S*Tm infection pathogenesis (Yoon et al 2009). Importantly, we identified a second SPI-2 effector gene network encoded by the *spv* operon that together with θ genes induced a lethal systemic infection in a mouse model of Typhoid fever (Fang et al 1991, Krause & Guiney 1991, Matsui et al 2001, Roudier et al 1992). The *spv* operon encodes three effector genes, *spvB-D*. SpvB ADP-ribosylates G-actin through a nicotinamide adenine dinucleotide (NAD)-dependent mechanism, thereby preventing F-actin polymerization (Tezcan-Merdol et al 2001). SpvC is a phosphothreonine lyase that inhibits mitogen-activated protein kinases (MAPK) through β-elimination of key phosphorylated threonine residues (Zhu et al 2007). Lastly, SpvD is a cysteine hydrolase that inhibits the NF-κB signaling pathway (Grabe et al 2016, Rolhion et al 2016). While it is currently unclear how these activities support *S*Tm pathogenesis, we suspect that at least part of the contribution of the *spv* locus is suppressing innate immune responses that are critical for *S*Tm to cross the mucosal membrane barrier.

A framework for adaptation of *Salmonella* to new environmental niches.

The genus *Salmonella* comprises over 2500 serovars that have co-evolved with animal hosts for millions of years. Comparative genomic analysis shows that the majority of θ genes required for intracellular replication of *S*Tm are highly conserved across *S. enterica* serovars (Jennings et al 2017). It therefore appears that host cell cytoplasm is strong environmental pressure driving the purifying selection of these SPI-2 effector genes (Jennings et al 2017, Johnson et al 2018, McClelland et al 2001, Nuccio & Baumler 2014). We also recognize the diversifying selection of effector genes, such as the acquisition of plasmid encoded *spv* operon by *S*Tm, has allowed *Salmonella* to adapt to new environmental challenges. Consistent with this idea, a combination of θ and *spvB-D* effector genes (*S*Tm Ω strain) was required for *Salmonella* to cause Typhoid like disease in C57BL/6 mice. In contrast, removal of the essential θ genes *sopD2* and *steA* needed for *Salmonella* to initiate SCV biogenesis prevented the *S*Tm Ω strain from colonizing host tissues. Interestingly, while this complement of genes is sufficient for infection of conventionally raised mice, *S*Tm Ω failed to cause disease in a model of *S*Tm-induced colitis or to colonize a naturally resistant mouse strain (Figure 6E). Thus, additional effector genes have been acquired for *S*Tm to occupy and/or combat immune cell types that are activated during Streptomycin treatment or that express high levels of Nramp1, respectively. Comparative genomics of naturally occurring variation in the *Salmonella* genus combined with phenotype guided genome engineering of the *S*Tm θ reference strain may provide an experimental avenue to unravel these complex mechanisms of bacterial pathogenesis.

Limitation of the study.

The conclusions drawn from this study are limited by the host models used to examine *S*Tm pathogenesis, including the human and mouse cell lines as well as the specific mouse strains. Future studies will be needed to determine if the θ gene network of *Salmonella* is required for survival in monocytes, neutrophils, dendritic cells, B- or T-cells *in vivo*. Additionally, it will be important to determine which other effector genes are required for *S*Tm to survive both acute and chronic immunological challenges presented by diverse mouse species (e.g. Nramp1^{+}). Finally, we recognize that the conclusions of this study are limited to the SL1344 strain of *S*Tm. Although the SPI-2 effector genes are highly conserved across the Typhimurium serovar, different strains can exhibit greater or lesser virulence. It will be important to determine how additional adaptations in these serovars have changed the requirements of SPI-2 effector proteins during the course of *Salmonella* evolution.

STAR METHODS

RESOURCE AVAILABILITY

LEAD CONTACT—Further information and requests for resources should be directed to and will be fulfilled by the Lead Contact, Neal M. Alto (neal.alto@utsouthwestern.edu).

MATERIALS AVAILABILITY—Plasmids, recombinant protein, experimental strains, and any other research reagents generated by the authors will be distributed upon request to other research investigators under a Material Transfer Agreement.

DATA AND CODE AVAILABILITY—This study did not generate/analyze unique datasets or code.

EXPERIMENTAL MODEL AND SUBJECT DETAILS

Bacteria -—*E. coli* and *Salmonella enterica* serovar Typhimurium SL1344 strains were grown aerobically at 37°C in LB broth (10 g/l tryptone, 5 g/l yeast extract, 10 g/l sodium chloride) or on LB agar plates (10 g/l tryptone, 5 g/l yeast extract, 10 g/l sodium chloride, 15 g/l agar). When appropriate, agar plates and media were supplemented with the following antibiotics at the indicated concentrations: ampicillin (100 μg/ml), kanamycin (50 μg/ml), streptomycin (100 μg/ml), carbenicillin (50 μg/ml), and chloramphenicol (30 μg/ml). *S*Tm strains expressing green fluorescent protein (GFP) or mCherry were constructed by electroporation of the bacteria with the pBBR1MCS 6Y (GFP expression)(Murphy et al 2002) or pDP151 (mcherry expression)(Burnaevskiy et al 2013) plasmids, respectively. To distinguish between *S*Tm strains used in the competition experiment, the chromogenic substrate 5-Bromo-4-chloro-3-indolyl phosphate (X-phos) (40 μg/ml) was added to agar plates to detect the activity of the acidic phosphatase PhoN.

Plasmids -—All plasmids used in this study are listed in the Key Resource Table. Standard Gibson cloning techniques were used to generate the plasmids used in this study. Suicide plasmids were routinely propagated in DH5α λpir.

Mammalian Cells -—Hela (human; sex: female, cervical epithelial), HCT116 (human; sex: male, colon epithelial), and Raw264.7 (mouse; macrophage) cells were grown in Dulbecco's Modified Eagle Medium (DMEM) high glucose, supplemented with 10% Fetal Bovine Serum (FBS). H1299 (human; sex: male, lung epithelial) cells were grown in RPMI 1640 with L-glutamine 10% FBS. T84 (human; sex: male, colon epithelial) cells were grown in DMEM/F12 media supplemented with 10% FBS. Hela and Raw264.7 cells were obtained from ATCC. HCT116, T84, H1299 cells were obtained from the Mendel lab, Winter lab, and Minna Lab at UTSW, respectively.

Mice -—C57BL/6 and 129X1/SvJ mice were purchased from the Jackson Laboratory. C57BL/6J mice homozygous for the *Nramp1*^{G169} allele (Arpaia et al 2011) were kindly provided by the Winter lab. Mice used for experiments were female 8–10 weeks old. All mice were maintained under pathogen-free conditions in the animal care facility at UT Southwestern Medical Center. All experiments were performed according to experimental protocols approved by the Institutional Animal Care and Use Committee and complied with all relevant ethical regulations.

METHODS DETAILS

Procedures for deleting individual SPI-2 effector genes from *S*Tm.—λ-red recombineering technology was used to replace effector genes with a kanamycin resistance (Kan^R) cassette as previously described (Datsenko & Wanner 2000). Briefly, mutagenesis primers were designed to amplify the Kan^R cassette from the pKD4 plasmid with 40-nucleotide sequences homologous to regions flanking the target gene on the chromosome. Primers were designed to preserve the first ten amino acids of the target gene to ensure

that regulatory elements were maintained. Primer sequences are listed in Table S1 in the supplemental material. After amplification of the targeting cassette, the linear double-stranded DNA was introduced by electroporation into *S*Tm cells harboring the λ-red recombinase expression plasmid pKD46. The linear DNA fragment was then integrated into the genome at a defined position by homologous recombination mediated by arabinose-induced activity of the λ-red system. To cure the Kan^R cassette from the newly generated *S*Tm mutant strains, *S*Tm strains were electroporated with pCP20, resulting in expression of FLP. FLP recognition of the FRT sites induced excision of the Kan^R cassette (Datsenko & Wanner 2000). Deletion of the target gene was confirmed by PCR.

Procedures for generating the SPI-2 polymutant library and *S*Tm Efl.—To generate *S*Tm SPI-2 polymutants and the effectorless strain (*S*Tm Efl), we first PCR amplified the region located between 500 and 1000 bp downstream of the effector gene stop codon. The resulting ~500 bp product was cloned into the vector pRDH10, a λpir-dependent suicide vector carrying *sacB* and a chloramphenicol resistance gene (Cm^R) (Kingsley et al 1999). The primer sequences used for generating the pRDH10-targeting constructs are shown in Table S2 in the supplemental material. Each pRDH10-targeting construct was introduced into each of the corresponding single deletion mutant strains by conjugation with the SM10 λpir donor strain. For example, the pRDH10 vector harboring ~500 bp sequence downstream of *pipAB* (plasmid pNA102) was transformed into SM10 λpir and then conjugated into *S*Tm Δ*pipAB* (strain NA102). The pRDH10 plasmid in *S*Tm was selected by plating the SM10 λpir and *S*TmΔ*pipAB* mixture on LB agar plates containing chloramphenicol and streptomycin (*S*Tm SL1344 is naturally resistant to streptomycin). Homologous recombination resulted in the integration of pRDH10 between 500 and 1000 bp downstream of the deleted *pipAB* locus (*S*Tm Δ*pipAB*::pRDH10). This procedure was performed on all 23 single gene deletion strains.

Phage P22 HT105 int lysates were generated from each individual effector gene knockout strain marked with pRDH10 using standard procedures (Schmieger 1972). The P22 lysate from *S*Tm Δ*pipAB*::pRDH10 was used to transduce the starting strain *S*Tm Δ*spvR* (Δ1). Phage transduction was performed as previously described (Schmieger 1972). Briefly, phage lysates were serially diluting by inoculating 10 μl of phage lysate into 90 μl PBS (3 serial dilutions were generated). Next, 100 μl of an overnight culture of the *S*Tm Δ1 starting strain was added to each of the diluted phage lysates and incubated at room temperature for 1 h. The mixture was spun at 12,000xg for 1 min at room temperature to pellet bacteria. The bacteria were resuspended in 100 μl PBS and plated on LB agar plates containing chloramphenicol to select *S*Tm Δ*spvR* Δ*pipAB*::pRDH10. To select for P22-free transductants, five to ten single colonies were first streaked on Evans Blue Uranine (EBU) plates (10 g/l Tryptone, 5 g/l Yeast Extract, 5 g/l NaCl, 2.5 g/l glucose, 15 g/l agar, 2.5 g/l K2HPO4, 0.00125% Evans Blue, and 0.0025% Sodium Fluorescein). White colonies were then tested for phage sensitivity by cross streaking against P22 H5 on EBU plates. Colonies resistant to P22 H5 were grown on LB agar plates. The pRDH10 plasmid was excised using sucrose counter selection by plating on sucrose plates (5 % sucrose, 15 g/l agar, 8 g/l nutrient broth base) as described (Lawes & Maloy 1995), thus generating strain *S*Tm Δ*spvR* Δ*pipAB* (Δ2).

This procedure was repeated in the order described in Table 1 to generate the polymutant library. Because of the close proximity between the *sseK2* and *steD* genes, we found that deletion of *sseK2* using phage-mediated recombination reintroduced the *steD* gene back into the *S*Tm Δ16 strain during the generation of the *S*Tm Efl strain (noted in Table 1). Therefore, *steD* was intact in all polymutant strains subsequent to *S*Tm Δ16. To eliminate *steD* from the final *S*Tm Efl strain, we first generated an *S*Tm Δ*steDsseK2* double using λ-red recombination as described above (see Table S1 for primer sequences). We then used p22 phage lysate obtained from this strain to knockout out *steD* from *S*Tm Efl as described above. Mutations in each of the 23 genomic loci encoding SPI-2 effectors in the *S*Tm Efl strain was confirmed by performing whole genome sequencing (Novogene) and by comparing the *S*Tm Efl sequence to both the wild-type *S*Tm SL1344 used in this study and the *S*Tm SL1344 reference genome (NC_016810.1). *S*Tm Efl exhibited copy number variation (CNV; large deletions) in each of the 22 genetic loci targeted, resulting in mutations in 27 SPI-2 effector genes and the *spvR* gene required for expression of *spvBCD*. *S*Tm Efl also carried a deletion in the *ccmH* gene (starting at nucleotide 4033901). This gene is non-essential and is a pseudogene in numerous *S. enterica* serovars. Four single nucleotide polymorphisms (SNPs) were identified in the *nrdH*, *murC*, *adeP*, *RS01300* genes in *S*Tm Efl, but not *S*Tm WT. In addition, two SNPs were identified in *menC* and *RSO2910* in both *S*Tm WT and *S*Tm Efl. None of these SNPs resulted in a non-sense mutation. Sequencing results are available upon request.

Engineering the *S*Tm Efl strain to express specific SPI-2 effector genes.— Prior to modifying the *S*Tm Efl strain, pRDH10 targeting constructs described above were integrated into *S*Tm WT to generate strains *S*Tm WT *spvR*::pRDH10, *S*Tm WT *sopD2*::pRDH10, *S*Tm WT *steA*::pRDH10, *S*Tm WT *sseFG*::pRDH10, and *S*Tm WT *sifA*::pRDH10. P22 Phage lysates were generated from each of these strains as described above. Next, these P22 phage lysates were used to repair specific effector gene mutations in *S*Tm Efl strain using the phage transduction procedure and genetic selection procedure described above. For example, P22 phage lysate from *S*Tm WT *spvR*::pRDH10 were used to repair the *spvR* mutation in the *S*Tm Efl strain resulting in *S*Tm Efl $spvR^{+}$ (NA102). All engineered strains were confirmed by PCR.

Deletion of *spvABCD* and complementation of *spvB/C*.—To delete *spvA*, *spvB*, *spvC*, or *spvD* in *S*Tm Ω strain by allelic exchange, 500 bp regions upstream of the start codon and 500 bp downstream of the stop codon of *spvA, spvB, spvC, and spvD* were PCR amplified from *Salmonella* Typhimurium strain SL1344 using the primers listed in Table S3. Gibson Assembly cloning kit (New England Biolabs) was used to clone the upstream and downstream regions into the suicide plasmid pRDH10. This generated plasmids pNA125, pNA126, pNA127, and pNA128. Plasmids were verified by sequencing. These suicide plasmids were routinely propagated in DH5α λpir and introduced into *S*Tm Ω by conjugation with the SM10 λpir donor strain. Clones with the appropriate integration of the suicide plasmid via a single crossover event were recovered on LB plates containing streptomycin and chloramphenicol. Subsequent sucrose selection was performed on sucrose plates (described above) to select for second crossover events leading to the unmarked

deletion of the target gene. The generated strains NA195, NA196, NA197, and NA198 were confirmed by PCR.

For *spvB* and *spvC* complementation, *spvB* and *spvC* were amplified with the primers listed in Table S3 and cloned into the plasmid pSW327 (Spiga et al 2017). This generated plasmids pNA129 and pNA130. Plasmids were verified by sequencing. These plasmids were introduced into NA196 or NA197 strains by conjugation with the SM10 λpir donor strain. The conjugates were selected by plating on LB plates containing streptomycin and carbenicillin. The generated strains NA199 and NA200 were verified by PCR for the insert of interest.

Measurement of *S*Tm growth in LB broth.—To measure *S*Tm growth *in vitro* (Figure S2A and S2B), bacterial cultures were initiated in LB broth with aeration (180rpm) overnight for 15 h at 37°C. The following day, overnight cultures were inoculated into 50 ml sterile LB in 500 ml flask at a 1:100 dilution and subsequently grown at 37°C with aeration. Samples were collected at different time points and diluted in sterile PBS for the measurements of the corresponding optical density at 600 nm or plated on LB agar plates for colony-forming units (CFUs).

STm infection of mammalian cells.—To prepare bacteria for infection, the *S*Tm strains were scraped from a glycerol stock into 10 ml LB broth containing appropriate antibiotics in a 250 ml flask and incubated overnight at 37°C with shaking. Bacterial cultures were then diluted 1:33 in 10 ml of fresh LB in a 250 ml flask and incubated at 37°C in a shaking incubator until the culture reaches OD600 of 0.6. The bacterial culture was spun at 4000 g for 2 min (room temperature), washed with cell culture medium, and then resuspended in 600 μl of culture medium.

Mammalian cells cultured in antibiotic free media were inoculated with *S*Tm to achieve the desired multiplicity of infection (MOI) as determined by serial diluting the bacterial cultures used for the infection. Cells were then centrifuged for 5 min at room temperature (800 g) to facilitate bacterial adherence and then incubated for 25 min at 37 °C in 5% CO_2. Cells were then washed with PBS for three times and incubated in medium containing 100μg/ml gentamicin for 1 h to kill extracellular bacteria. Quantification of *S*Tm invasion was performed at this stage as described below. For subsequent analysis of intracellular *S*Tm replication and SCV morphology, the concentration of gentamicin was reduced to 10 μg/ml and cells were incubated for an additional 16.5 h (37 °C, 5% CO_2).

For the quantification of *S*Tm invasion in H1299 cells and Hela cells, cells were seeded in 24-well plates at a density of 1×10^5 per well 24 h before infection and infected at MOI of 100 as describe above. Inoculated CFUs were determined by serial dilutions of bacterial culture used for the infection. Cells were lysed with 0.5% Triton X-100 at 1.5 hour post infection (h p.i.) and serial dilutions were plated to enumerate the CFUs as described above. Invasion capacity was determined by dividing the CFUs recovered at 1.5 h p.i. by the number of the original inoculum.

For the quantification of *S*Tm replication by CFUs in epithelial cells (e.g. Figure 1B), cells were seeded in 24-well plates at a density of 1×10^5 per well 24 h before infection and infected at MOI of 40. Medium was removed at 1.5 h p.i. or 18 h p.i. and the cells were washed 3 times in PBS and lysed in 0.5% Triton X-100 for 10 min at room temperature, followed by vigorous pipetting to complete the lysis. Samples were serially diluted, plated on LB agar plates and incubated overnight at 37 °C. Colonies were counted. The fold of replication was calculated as the number of CFUs recovered at 18 h p.i. by the CFUs recovered at 1.5 h p.i..

For the quantification of survival index by CFUs in murine macrophage RAW264.7 cells (e.g. Figure 1D), RAW264.7 cells were seeded in 24-well plates at a density of 2×10^5 per well 24 h before infection and infected at MOI of approximately 10 as described above. Cells were lysed with 0.5% Triton X-100 and serial dilutions were plated to enumerate the CFUs as described above. In each experiment, values of mean fold change in number of CFUs between 1.5 h p.i. and 18 h p.i. were calculated and normalized to that of the wild-type strain to obtain a survival index, which, for the wild-type strain, was 1.0.

Imaging *S*Tm by widefield and confocal microscopy.

For imaging *S*Tm infection in H1299 cells by widefield fluorescence microscopy (e.g. Figure 1C), cells were seeded on glass coverslips in 24-well plates at a density of 5×10^4 cells per well 24 h before infection and infected at MOI of 25 for 18 h as described above. Cells were washed three times in PBS and fixed in 3.7% formaldehyde for 10 min. Cell were then permeabilized with 0.5% Triton X-100 for 5 min and incubated for 5 min in 4', 6-diamidino-2-phenylindole (DAPI). Cells were then washed with distilled water for 3 times. Coverslips were mounted on slides with Prolong Glass mounting media (Invitrogen P369870).

For quantification of bacteria number per cell in H1299 cells (e.g. Figure 3A), samples were prepared for imaging by wide field fluorescence microscopy as described below. The number of internalized bacteria per cell was determined by manual count. Cells infected with more than 100 bacteria were scored as ">100".

For imaging the SCV in *S*Tm infected H1299 and Hela cells by widefield or confocal microscopy as indicated in the figure legend, cells were plated on glass coverslips and infected with *S*Tm as described above for 18 h, washed with PBS for 3 times, and then fixed with 3.5% PFA for 20 min. The fixed cells were washed with PBS for 3 times. All the subsequent steps were done with slow rocking. Cells were incubated in blocking buffer (PBS containing 0.1% saponin and 2% BSA) for 30 min. Permeabilized cells were stained with the primary antibody mouse anti-human Lamp1 (abcam, ab25630, 1:250 in blocking buffer) for 1h at room temperature. Cells were washed with PBS for 6 times and incubated with secondary antibody (e.g. goat anti-mouse, Rhodamine or goat anti-mouse 647) diluted 1:200 in blocking buffer for 1 h at room temperature. Cells were washed with PBS for 6 times, stained with DAPI and washed with distilled water as described above. Coverslips were mounted on slides with Prolong Glass mounting media.

For imaging *S*Tm strains in the co-infection trans-complementation assay in H1299 cells (Figure S3 and Figure 4D–F) by wide field fluorescence or confocal microscopy as indicated, H1299 cells were infected with the 1:1 mixture of GFP-expressing *S*Tm and mCherry-expressing *S*Tm in each group with a total MOI of 50 as described above. Cells were fixed at 18 h p.i. and stained for endogenous Lamp1. For Figure S3, the number of internalized bacteria per cell was scored for two types of cells, cells infected with GFP-expressing *S*Tm only, and cells infected with both GFP-expressing *S*Tm and mCherry-expressing *S*Tm. 50 infected cells were scored for each strain from two independent experiments.

For widefield fluorescence microscopy, cells were imaged on a Zeiss Observer.Z1 inverted microscope at 63x (Plan-Apochromat 63x/1.4 Oil objective). For confocal microscopy, cells were imaged on either a Zeiss LSM 780 or 880 inverted confocal microscope at 40x (Plan-Apochromat 40x/1.4 Oil objective) using 405, 488 and 561 lasers for excitation of DAPI, GFP and Rhodamine, respectively. Images are single z-planes with an optical section thickness of 1 μm.

Transmission Electron Microscopy of *S*Tm infected cells.

For Transmission electron microscopy (TEM) analysis, H1299 cells were seeded on MatTek dishes and infected at MOI of 25 for 18 h as described above. Cells were fixed with 2.5% (v/v) glutaraldehyde in 0.1M sodium cacodylate buffer. After three rinses in 0.1M sodium cacodylate buffer, they were post-fixed in 1% osmium tetroxide and 0.8 % K3 [Fe (CN6)] in 0.1M sodium cacodylate buffer for 1 h at room temperature. Samples were rinsed with water and en bloc stained with 2% aqueous uranyl acetate overnight. After three rinses with water, they were dehydrated with increasing concentration of ethanol, infiltrated with Embed-812 resin and polymerized in a 60°C oven overnight. Blocks were sectioned with a diamond knife (Diatome) on a Leica Ultracut UC7 ultramicrotome (Leica Microsystems) and collected onto copper grids, post stained with 2% Uranyl acetate in water and lead citrate. Images were acquired on a JEOL 1400 Plus (JEOL) equipped with a LaB6 source using a voltage of 120 kV.

*S*Tm infection of mice.

8–10 weeks old C57BL/6, 129X1/SvJ, and C57BL/6 *Nramp1*^{G169} (Arpaia et al 2011) mice were maintained under pathogen-free conditions in the animal care facility at UT Southwestern Medical Center. For *S*Tm intravenous (i.v.) infections (e.g. Figure 1E), *S*Tm strains were cultured to log-phase growth in brain heart infusion broth at 37°C, washed and diluted with sterile saline, and injected intravenously through the lateral tail vein at 10^3 CFUs per mouse. For *S*Tm oral infection, *S*Tm strains were grown overnight in LB broth supplemented with 100 μg/ml streptomycin in a shaker at 37°C and then diluted to 10^9 CFUs in 0.1 ml LB. *S*Tm strains were loaded in a feeding needle and delivered to mice by gavage. Bacterial loads in different tissues were determined by homogenizing organs in 5 ml PBS and by plating serial dilutions on LB plates containing streptomycin. For survival experiments, mice were monitored daily for 2 weeks. Mice that exhibited a weight loss of greater than 20% of their starting weight were euthanized via carbon dioxide followed by cervical dislocation.

For immunophenotyping of orally infected mice (Figure 5B), C57BL/6 mice were orally infected with approximately 10^9 CFUs of *S*Tm strains as described above. To determine immune cell counts in the spleen, mice were sacrificed 4 days post infection and spleens were mechanically homogenized though a 70 μm cell strainer (Falcon) with a 1 ml Plastic syringe (BD Biosciences) into 5 ml R1 buffer (RPMI with 5% FBS). The homogenized filter was washed with 15 ml R1 buffer and passed through the filter once again. Cells were pelleted (450xg, 4°C, 5 min). Red blood cells were lysed with 2 ml RBC lysis buffer and incubated on ice for 5 min. Chilled PBS was added for a final volume of 20 ml. Cells were pelleted and resuspended in 1 ml chilled PBS. 4×10^6 cells were plated for technical replicates and controls into 96 well TC-treated V-bottom plates (Corning) and pelleted. Single cell suspensions were incubated in 50 μl Ghost Dye Violet 450 diluted 50x in PBS at 4°C for 30 min in the dark. After incubation, cells were resuspended in 100 μl FACS buffer (PBS with 3%FBS). Cells were pelleted and resuspended in 50 μl 1:100 Fc Shield at 4°C for 20 min in the dark. 100 μl FACS buffer was added and the cells were pelleted then stained with antibodies for surface antigens. Cells were washed with 150 μl FACS buffer and incubated with 1% PFA for 20 min. Cells were pelleted again and resuspended in 100 μl FACS buffer. Cells were then analyzed on the S1000EX flow cytometer (Stratedigm). Data was acquired using CellCapTure software (Stratedigm) and analyzed with FLowJo software (TreeStar). Details of reagents used were shown in Table S4.

To examine *S*Tm persistence (Figure 6D and Figure S6), C57BL/6 mice carrying the *Nramp1*^{G169} allele (Arpaia et al 2011) or 129X1/SvJ mice were infected orally as described above. Mice were sacrificed 21 days post infection and organs were collected to determine bacterial loads as described above.

For competition experiments (Figure 5C), mice were administered 5×10^8 CFUs of the WT (Δ*phoN*) strain (SW759) (Winter et al 2014) and 5×10^8 CFUs of the competing strain orally as described above. To determine bacterial loads in the spleens and livers, mice were sacrificed 4 days post infection, organs were homogenized in sterile PBS and serial dilutions were plated on selective agar plates to determine CFUs of each *S*Tm strain. Competitive indices were calculated on CFU/g as (mutant output/ WT (Δ*phoN*) output)/(mutant input/ WT (Δ*phoN*) input). Samples with bacteria below the limit of detection were assigned a value of 1 per mouse in the calculation of competitive indices.

For streptomycin treatment of mice (e.g. Figure 6A), water and food were withdrawn for 8–10 weeks old C57BL/6 mice for 4 h before oral administration with 20 mg of streptomycin dissolved in 100 μl sterile water. Afterward, animals were supplied with water and food. 24 h post streptomycin treatment, the mice were orally inoculated with 10^9 CFUs of *S*Tm as described above. Mice were sacrificed at 4 days or 15 days (for *S*Tm θ and *S*Tm Ω) post infection and organs were collected to determine bacterial loads as described above. For survival experiments, mice were monitored daily for 2 weeks as described above.

Quantification and statistical analysis.

GraphPad Prism 8 was used for graph preparation and statistical analysis. Data were represented as mean ± SEM (standard error of the mean). Figure 1B, 1D, 1F, 2D, 3A, 5A, and 5E: Statistical significance in comparison to *S*Tm WT was determined using the one-

way analysis of variance (ANOVA). Figure 2C, 6B, and 6D: Statistical significance between groups was determined using the one-way ANOVA. Unless specified, comparisons were made with *S*Tm WT. Figure 5F, 6C: Statistical significance was determined using Student's t test. The significance level was represented by asterisks: *, $0.01<p<0.05$. **, $p<0.01$. ***, $p<0.001$. ****, $p<0.0001$. ns, $p>0.05$. The exact number of independent samples (N) and other information regarding descriptive statistics is listed in each figure legend.

Supplementary Material

Refer to Web version on PubMed Central for supplementary material.

ACKNOWLEDGEMENTS

We would like to thank members of the Alto laboratory for helpful discussions. We acknowledge the assistance of the UT Southwestern Electron Microscopy Core, especially Katherine Luby-Phelps (supported by NIH grant 1S10OD021685–01A1). This research was supported by grants from the National Institutes of Health (grant no. AI118807 to S.E.W., DP1AI131080 to S.S.W., and AI083359 to N.M.A.), The Welch Foundation (grant no. I-1704 to N.M.A.), the Burroughs Welcome Fund (grant no. 1017880 to S.E.W., 1011031 to S.S.W., and 1011019 to N.M.A.) and the Howard Hughes Medical Institute and Simons Foundation Faculty Scholars Program (grant no. 55108587 to S.S.W. and 55108499 to N.M.A).

REFERENCES

Arpaia N, Godec J, Lau L, Sivick KE, McLaughlin LM, et al. 2011. TLR signaling is required for Salmonella typhimurium virulence. Cell 144: 675–88 [PubMed: 21376231]

Barthel M, Hapfelmeier S, Quintanilla-Martinez L, Kremer M, Rohde M, et al. 2003. Pretreatment of mice with streptomycin provides a Salmonella enterica serovar Typhimurium colitis model that allows analysis of both pathogen and host. Infect Immun 71: 2839–58 [PubMed: 12704158]

Beuzon CR, Meresse S, Unsworth KE, Ruiz-Albert J, Garvis S, et al. 2000. Salmonella maintains the integrity of its intracellular vacuole through the action of SifA. The EMBO journal 19: 3235–49 [PubMed: 10880437]

Beuzon CR, Salcedo SP, Holden DW. 2002. Growth and killing of a Salmonella enterica serovar Typhimurium sifA mutant strain in the cytosol of different host cell lines. Microbiology 148: 2705–15 [PubMed: 12213917]

Boucrot E, Henry T, Borg JP, Gorvel JP, Meresse S. 2005. The intracellular fate of Salmonella depends on the recruitment of kinesin. Science 308: 1174–8 [PubMed: 15905402]

Bruno VM, Hannemann S, Lara-Tejero M, Flavell RA, Kleinstein SH, Galan JE. 2009. Salmonella Typhimurium type III secretion effectors stimulate innate immune responses in cultured epithelial cells. PLoS Pathog 5: e1000538 [PubMed: 19662166]

Buchmeier NA, Heffron F. 1991. Inhibition of macrophage phagosome-lysosome fusion by Salmonella typhimurium. Infect Immun 59: 2232–8 [PubMed: 2050395]

Burnaevskiy N, Fox TG, Plymire DA, Ertelt JM, Weigele BA, et al. 2013. Proteolytic elimination of N-myristoyl modifications by the Shigella virulence factor IpaJ. Nature 496: 106–9 [PubMed: 23535599]

Cirillo DM, Valdivia RH, Monack DM, Falkow S. 1998. Macrophage-dependent induction of the Salmonella pathogenicity island 2 type III secretion system and its role in intracellular survival. Molecular microbiology 30: 175–88 [PubMed: 9786194]

Cunnac S, Chakravarthy S, Kvitko BH, Russell AB, Martin GB, Collmer A. 2011. Genetic disassembly and combinatorial reassembly identify a minimal functional repertoire of type III effectors in Pseudomonas syringae. Proc Natl Acad Sci U S A 108: 2975–80 [PubMed: 21282655]

D'Costa VM, Braun V, Landekic M, Shi R, Proteau A, et al. 2015. Salmonella Disrupts Host Endocytic Trafficking by SopD2-Mediated Inhibition of Rab7. Cell Rep 12: 1508–18 [PubMed: 26299973]

Datsenko KA, Wanner BL. 2000. One-step inactivation of chromosomal genes in Escherichia coli K-12 using PCR products. Proceedings of the National Academy of Sciences of the United States of America 97: 6640–5 [PubMed: 10829079]

Deiwick J, Salcedo SP, Boucrot E, Gilliland SM, Henry T, et al. 2006. The translocated Salmonella effector proteins SseF and SseG interact and are required to establish an intracellular replication niche. Infection and immunity 74: 6965–72 [PubMed: 17015457]

Domingues L, Holden DW, Mota LJ. 2014. The Salmonella effector SteA contributes to the control of membrane dynamics of Salmonella-containing vacuoles. Infect Immun 82: 2923–34 [PubMed: 24778114]

Eswarappa SM, Negi VD, Chakraborty S, Chandrasekhar Sagar BK, Chakravortty D. 2010. Division of the Salmonella-containing vacuole and depletion of acidic lysosomes in Salmonella-infected host cells are novel strategies of Salmonella enterica to avoid lysosomes. Infect Immun 78: 68–79 [PubMed: 19858305]

Fang FC, Krause M, Roudier C, Fierer J, Guiney DG. 1991. Growth regulation of a Salmonella plasmid gene essential for virulence. Journal of bacteriology 173: 6783–9 [PubMed: 1938884]

Forster AC, Church GM. 2006. Towards synthesis of a minimal cell. Mol Syst Biol 2: 45 [PubMed: 16924266]

Gibson DG, Benders GA, Andrews-Pfannkoch C, Denisova EA, Baden-Tillson H, et al. 2008. Complete chemical synthesis, assembly, and cloning of a Mycoplasma genitalium genome. Science 319: 1215–20 [PubMed: 18218864]

Gil R, Silva FJ, Pereto J, Moya A. 2004. Determination of the core of a minimal bacterial gene set. Microbiology and molecular biology reviews : MMBR 68: 518–37, table of contents [PubMed: 15353568]

Glass JI, Assad-Garcia N, Alperovich N, Yooseph S, Lewis MR, et al. 2006. Essential genes of a minimal bacterium. Proc Natl Acad Sci U S A 103: 425–30 [PubMed: 16407165]

Grabe GJ, Zhang Y, Przydacz M, Rolhion N, Yang Y, et al. 2016. The Salmonella Effector SpvD Is a Cysteine Hydrolase with a Serovar-specific Polymorphism Influencing Catalytic Activity, Suppression of Immune Responses, and Bacterial Virulence. J Biol Chem 291: 25853–63 [PubMed: 27789710]

Guiney DG, Fierer J. 2011. The Role of the spv Genes in Salmonella Pathogenesis. Frontiers in microbiology 2: 129 [PubMed: 21716657]

Hensel M, Shea JE, Waterman SR, Mundy R, Nikolaus T, et al. 1998. Genes encoding putative effector proteins of the type III secretion system of Salmonella pathogenicity island 2 are required for bacterial virulence and proliferation in macrophages. Mol Microbiol 30: 163–74 [PubMed: 9786193]

Hoiseth SK, Stocker BA. 1981. Aromatic-dependent Salmonella typhimurium are non-virulent and effective as live vaccines. Nature 291: 238–9 [PubMed: 7015147]

Holden DW. 2002. Trafficking of the Salmonella vacuole in macrophages. Traffic 3: 161–9 [PubMed: 11886586]

Hutchison CA 3rd, Chuang RY, Noskov VN, N Assad-Garcia, Deerinck TJ, et al. 2016. Design and synthesis of a minimal bacterial genome. Science 351: aad6253 [PubMed: 27013737]

Jennings E, Thurston TLM, Holden DW. 2017. Salmonella SPI-2 Type III Secretion System Effectors: Molecular Mechanisms And Physiological Consequences. Cell host & microbe 22: 217–31 [PubMed: 28799907]

Johnson R, Mylona E, Frankel G. 2018. Typhoidal Salmonella: Distinctive virulence factors and pathogenesis. Cellular microbiology 20: e12939 [PubMed: 30030897]

Jones BD, Falkow S. 1996. Salmonellosis: host immune responses and bacterial virulence determinants. Annual review of immunology 14: 533–61

Kingsley RA, Reissbrodt R, Rabsch W, Ketley JM, Tsolis RM, et al. 1999. Ferrioxamine-mediated Iron(III) utilization by Salmonella enterica. Appl Environ Microbiol 65: 1610–8 [PubMed: 10103258]

Knuff-Janzen K, Tupin A, Yurist-Doutsch S, Rowland JL, Finlay BB. 2020. Multiple Salmonella-pathogenicity island 2 effectors are required to facilitate bacterial establishment of its intracellular niche and virulence. PLoS One 15: e0235020 [PubMed: 32584855]

Krause M, Guiney DG. 1991. Identification of a multimer resolution system involved in stabilization of the Salmonella dublin virulence plasmid pSDL2. Journal of bacteriology 173: 5754–62 [PubMed: 1653217]

Lawes M, Maloy S. 1995. MudSacI, a transposon with strong selectable and counterselectable markers: use for rapid mapping of chromosomal mutations in Salmonella typhimurium. J Bacteriol 177: 1383–7 [PubMed: 7868615]

Matsuda S, Haneda T, Saito H, Miki T, Okada N. 2019. Salmonella enterica Effectors SifA, SpvB, SseF, SseJ, and SteA Contribute to Type III Secretion System 1-Independent Inflammation in a Streptomycin-Pretreated Mouse Model of Colitis. Infect Immun 87

Matsui H, Bacot CM, Garlington WA, Doyle TJ, Roberts S, Gulig PA. 2001. Virulence plasmid-borne spvB and spvC genes can replace the 90-kilobase plasmid in conferring virulence to Salmonella enterica serovar Typhimurium in subcutaneously inoculated mice. J Bacteriol 183: 4652–8 [PubMed: 11443102]

McClelland M, Sanderson KE, Spieth J, Clifton SW, Latreille P, et al. 2001. Complete genome sequence of Salmonella enterica serovar Typhimurium LT2. Nature 413: 852–6 [PubMed: 11677609]

McGourty K, Thurston TL, Matthews SA, Pinaud L, Mota LJ, Holden DW. 2012. Salmonella inhibits retrograde trafficking of mannose-6-phosphate receptors and lysosome function. Science 338: 963–7 [PubMed: 23162002]

Monack DM, Bouley DM, Falkow S. 2004. Salmonella typhimurium persists within macrophages in the mesenteric lymph nodes of chronically infected Nramp1+/+ mice and can be reactivated by IFNgamma neutralization. J Exp Med 199: 231–41 [PubMed: 14734525]

Muller AJ, Kaiser P, Dittmar KE, Weber TC, Haueter S, et al. 2012. Salmonella gut invasion involves TTSS-2-dependent epithelial traversal, basolateral exit, and uptake by epithelium-sampling lamina propria phagocytes. Cell Host Microbe 11: 19–32 [PubMed: 22264510]

Murphy E, Robertson GT, Parent M, Hagius SD, Roop RM 2nd, et al. 2002. Major histocompatibility complex class I and II expression on macrophages containing a virulent strain of Brucella abortus measured using green fluorescent protein-expressing brucellae and flow cytometry. FEMS Immunol Med Microbiol 33: 191–200 [PubMed: 12110481]

Mushegian AR, Koonin EV. 1996. A minimal gene set for cellular life derived by comparison of complete bacterial genomes. Proc Natl Acad Sci U S A 93: 10268–73 [PubMed: 8816789]

Nuccio SP, Baumler AJ. 2014. Comparative analysis of Salmonella genomes identifies a metabolic network for escalating growth in the inflamed gut. mBio 5: e00929–14 [PubMed: 24643865]

Ochman H, Soncini FC, Solomon F, Groisman EA. 1996. Identification of a pathogenicity island required for Salmonella survival in host cells. Proc Natl Acad Sci U S A 93: 7800–4 [PubMed: 8755556]

Ohlson MB, Huang Z, Alto NM, Blanc MP, Dixon JE, et al. 2008. Structure and function of Salmonella SifA indicate that its interactions with SKIP, SseJ, and RhoA family GTPases induce endosomal tubulation. Cell Host Microbe 4: 434–46 [PubMed: 18996344]

Pal D, Venkova-Canova T, Srivastava P, Chattoraj DK. 2005. Multipartite regulation of rctB, the replication initiator gene of Vibrio cholerae chromosome II. J Bacteriol 187: 7167–75 [PubMed: 16237000]

Patel JC, Galan JE. 2005. Manipulation of the host actin cytoskeleton by Salmonella--all in the name of entry. Curr Opin Microbiol 8: 10–5 [PubMed: 15694851]

Simon R, Priefer U, and Puhler A (1983). A broad host range mobilization system for in vivo genetic engineering: transposon mutagenesis in Gram-negative bacteria. Biol. Technology 1, 784–791.

Rolhion N, Furniss RC, Grabe G, Ryan A, Liu M, et al. 2016. Inhibition of Nuclear Transport of NF-kB p65 by the Salmonella Type III Secretion System Effector SpvD. PLoS Pathog 12: e1005653 [PubMed: 27232334]

Roudier C, Fierer J, Guiney DG. 1992. Characterization of translation termination mutations in the spv operon of the Salmonella virulence plasmid pSDL2. Journal of bacteriology 174: 6418–23 [PubMed: 1400193]

Ruano-Gallego D, Sanchez-Garrido J, Kozik Z, Nunez-Berrueco E, Cepeda-Molero M, et al. 2021. Type III secretion system effectors form robust and flexible intracellular virulence networks. Science 371

Salcedo SP, Holden DW. 2003. SseG, a virulence protein that targets Salmonella to the Golgi network. The EMBO journal 22: 5003–14 [PubMed: 14517239]

Schmieger H 1972. Phage P22-mutants with increased or decreased transduction abilities. Mol Gen Genet 119: 75–88 [PubMed: 4564719]

Shea JE, Beuzon CR, Gleeson C, Mundy R, Holden DW. 1999. Influence of the Salmonella typhimurium pathogenicity island 2 type III secretion system on bacterial growth in the mouse. Infect Immun 67: 213–9 [PubMed: 9864218]

Shea JE, Hensel M, Gleeson C, Holden DW. 1996. Identification of a virulence locus encoding a second type III secretion system in Salmonella typhimurium. Proceedings of the National Academy of Sciences of the United States of America 93: 2593–7 [PubMed: 8637919]

Spano S, Gao X, Hannemann S, Lara-Tejero M, Galan JE. 2016. A Bacterial Pathogen Targets a Host Rab-Family GTPase Defense Pathway with a GAP. Cell Host Microbe 19: 216–26 [PubMed: 26867180]

Spiga L, Winter MG, Furtado de Carvalho T, Zhu W, Hughes ER, et al. 2017. An Oxidative Central Metabolism Enables Salmonella to Utilize Microbiota-Derived Succinate. Cell Host Microbe 22: 291–301 e6 [PubMed: 28844888]

Tezcan-Merdol D, Nyman T, Lindberg U, Haag F, Koch-Nolte F, Rhen M. 2001. Actin is ADP-ribosylated by the Salmonella enterica virulence-associated protein SpvB. Molecular microbiology 39: 606–19 [PubMed: 11169102]

Vazquez-Torres A, Jones-Carson J, Baumler AJ, Falkow S, Valdivia R, et al. 1999. Extraintestinal dissemination of Salmonella by CD18-expressing phagocytes. Nature 401: 804–8 [PubMed: 10548107]

Wei HL, Chakravarthy S, Mathieu J, Helmann TC, Stodghill P, et al. 2015. Pseudomonas syringae pv. tomato DC3000 Type III Secretion Effector Polymutants Reveal an Interplay between HopAD1 and AvrPtoB. Cell Host Microbe 17: 752–62 [PubMed: 26067603]

Weigele BA, Orchard RC, Jimenez A, Cox GW, Alto NM. 2017. A systematic exploration of the interactions between bacterial effector proteins and host cell membranes. Nat Commun 8: 532 [PubMed: 28912547]

Winter SE, Winter MG, Poon V, Keestra AM, Sterzenbach T, et al. 2014. Salmonella enterica Serovar Typhi conceals the invasion-associated type three secretion system from the innate immune system by gene regulation. PLoS Pathog 10: e1004207 [PubMed: 24992093]

Yoon H, McDermott JE, Porwollik S, McClelland M, Heffron F. 2009. Coordinated regulation of virulence during systemic infection of Salmonella enterica serovar Typhimurium. PLoS Pathog 5: e1000306 [PubMed: 19229334]

Yu XJ, Liu M, Holden DW. 2016. Salmonella Effectors SseF and SseG Interact with Mammalian Protein ACBD3 (GCP60) To Anchor Salmonella-Containing Vacuoles at the Golgi Network. mBio 7

Zhang K, Riba A, Nietschke M, Torow N, Repnik U, et al. 2018. Minimal SPI1-T3SS effector requirement for Salmonella enterocyte invasion and intracellular proliferation in vivo. PLoS Pathog 14: e1006925 [PubMed: 29522566]

Zhu Y, Li H, Long C, Hu L, Xu H, et al. 2007. Structural insights into the enzymatic mechanism of the pathogenic MAPK phosphothreonine lyase. Molecular cell 28: 899–913 [PubMed: 18060821]

Highlights

- Genome reconstruction reveals essential SPI-2 effector genes of *Salmonella*.
- A five gene network (θ genes) coordinates SCV division and *Salmonella* proliferation.
- θ genes and the *spv* operon cooperate to induce Typhoid fever in mice.
- Host tissue tropism is determined by diverse effector gene networks.

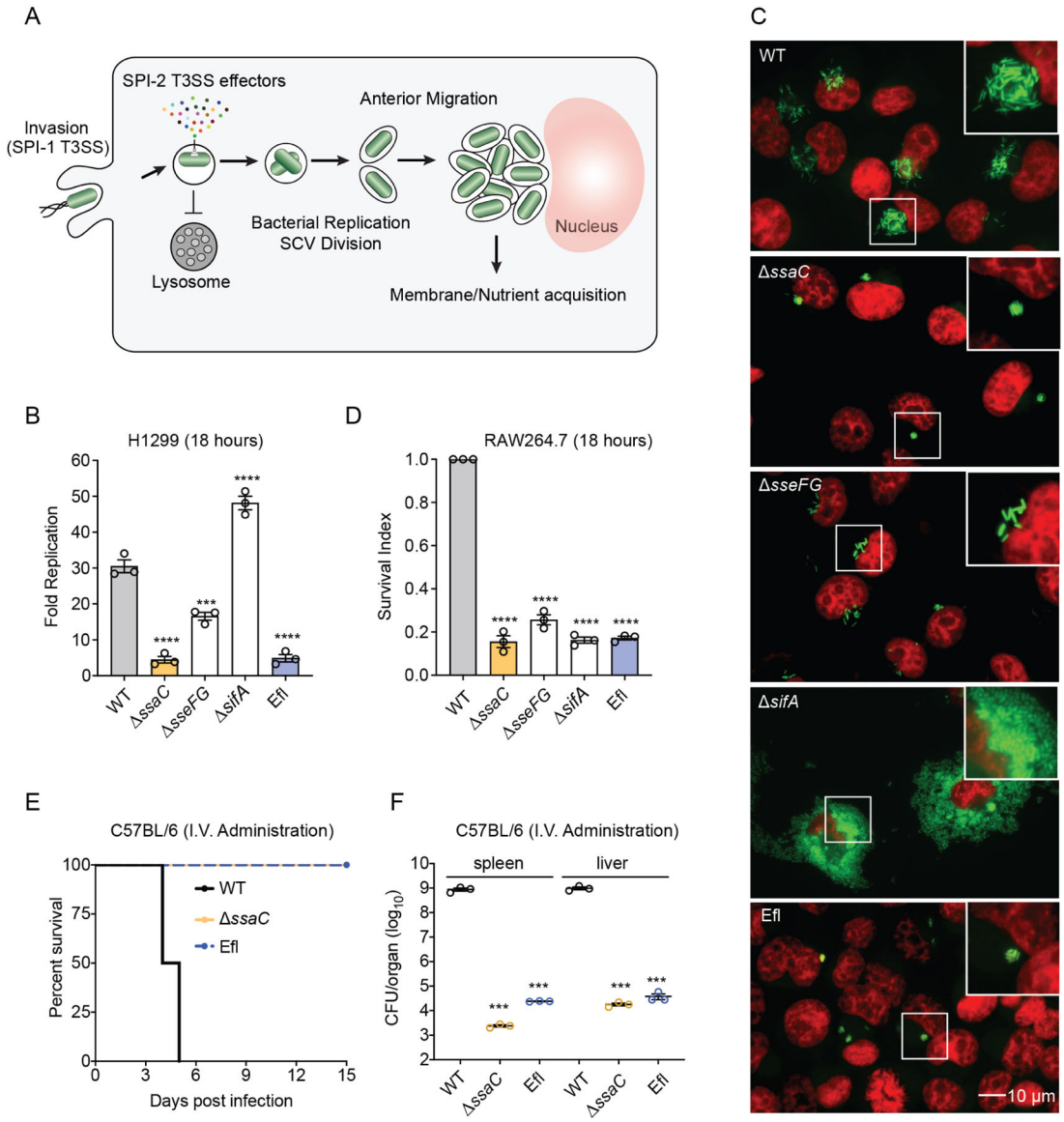

Figure 1 |. *S*Tm Efl phenocopies the SPI-2 T3SS deletion strain.

(A) Cartoon depiction of the *S*Tm intracellular lifecycle in epithelial cells.

(B) Fold replication of the *S*Tm strains indicated in H1299 cells. Fold change was calculated as CFUs recovered from lysed cells at 18 h p.i. versus CFUs recovered from lysed cells at 1.5 h p.i..

(C) Widefield fluorescence microscopy images of H1299 cells infected with the indicated GFP-expressing *S*Tm strains. Cells were fixed at 18 h p.i. and stained with DAPI (red). A higher magnification of the boxed area is shown at the upper right corner of each image.

(D) Survival index of different *S*Tm strains in RAW264.7 macrophages. Survival index was calculated as the ratio of CFUs recovered from lysed cells at 18 h p.i. to CFUs at 1.5 h p.i. and was normalized to *S*Tm WT values.

(E) C57BL/6 mice were infected intravenously and survival rates were followed for 15 days. Data are from 8 mice per group in two independent cohorts.

(F) Bacterial burden in spleen and liver were evaluated in intravenously infected C57BL/6 mice at 4 days post infection. Graph shows the average CFU per organ from three mice and is representative of 3 independent cohorts. Error bars show SEM (standard error of the mean). Statistical significance in comparison to *S*Tm WT was determined using the one-way analysis of variance (ANOVA). (***, $p<0.001$).

For (B) and (D), the bars represent the mean values. The error bars show the SEM from three independent experiments and statistical significance in comparison to *S*Tm WT was determined using the one-way ANOVA. (***, $p<0.001$.****, $p<0.0001$).

See also Figure S1 and Figure S2A–2D.

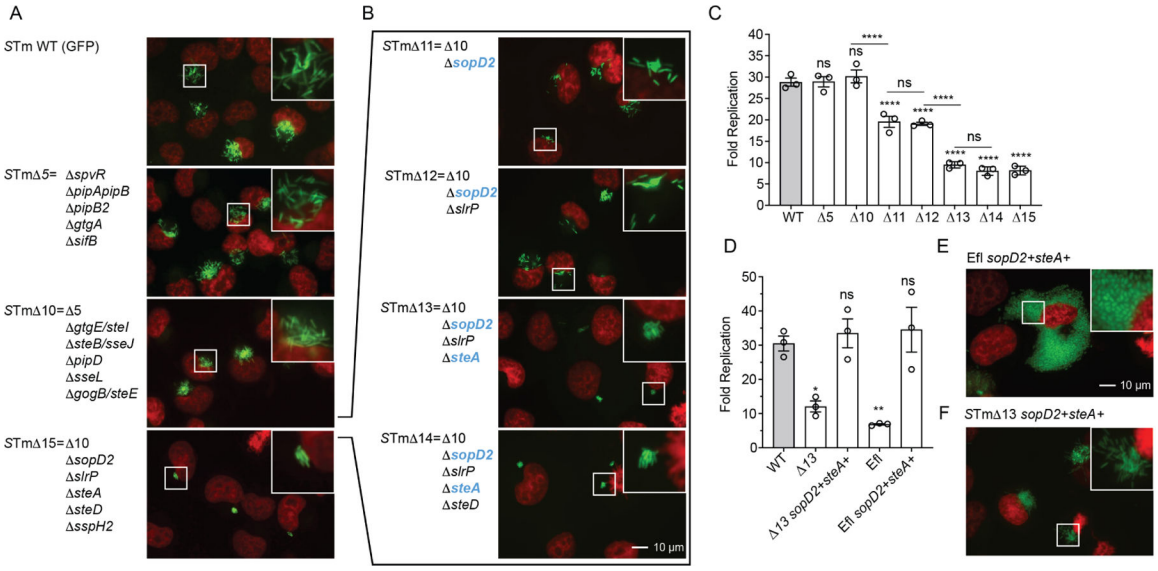

Figure 2 |. Identification of *sopD2* and *steA* as essential effector genes.

(A, B, E, and F) Widefield fluorescence microscopy images of H1299 cells infected with GFP-expressing *S*Tm strains as in Figure 1C.

(C-D) Fold replication of the indicated *S*Tm strains in H1299 cells. The fold change calculation was determined as in Figure 1B. Statistical significance was determined using the one-way ANOVA. Unless specified, comparisons were made with *S*Tm WT. (*, 0.01<p<0.05. **, p<0.01. ****, p<0.0001. ns, p>0.05).

See also Figure S2E–F.

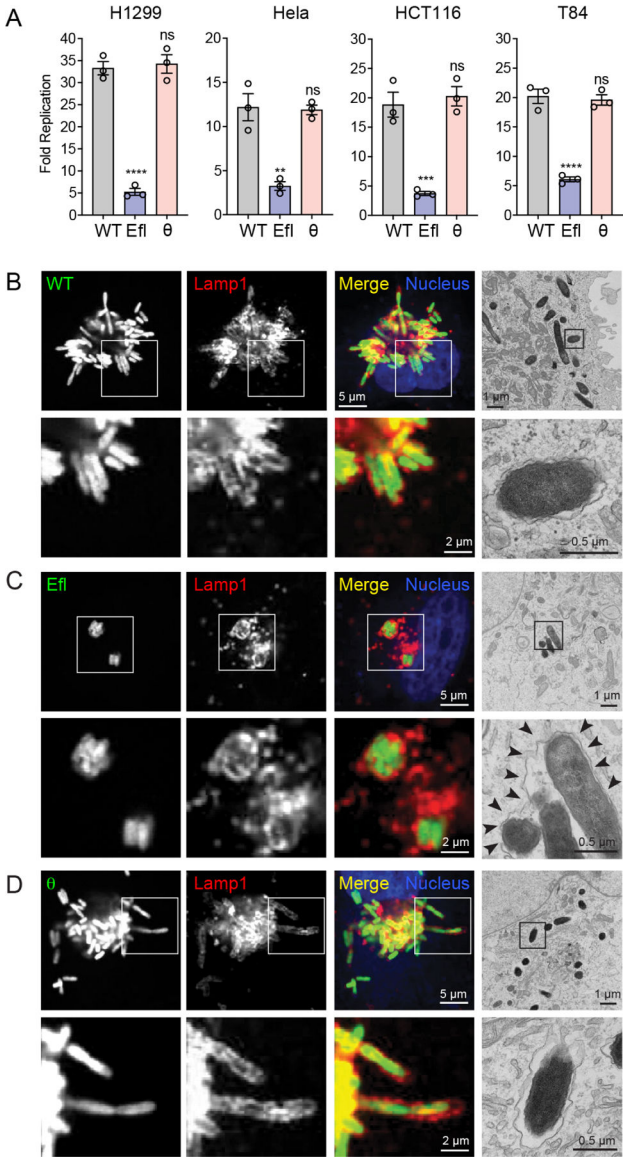

Figure 3 |. Identification of a minimal effector gene network that supports intracellular *Salmonella* replication and macrophage survival *in vitro*.

(A) Fold replication of the indicated *S*Tm strains in infected H1299, Hela, HCT116, and T84 cells and statistical significance was determined as in Figure 1B.

(B-D) Confocal microscopy and TEM images of H1299 cells infected with the indicated GFP-expressing *S*Tm strains for 18 h. The nucleus (blue) and endogenous Lamp1 (red) are shown. Arrowheads show the SCV membrane with multiple bacteria enclosed.

See also Figure S3.

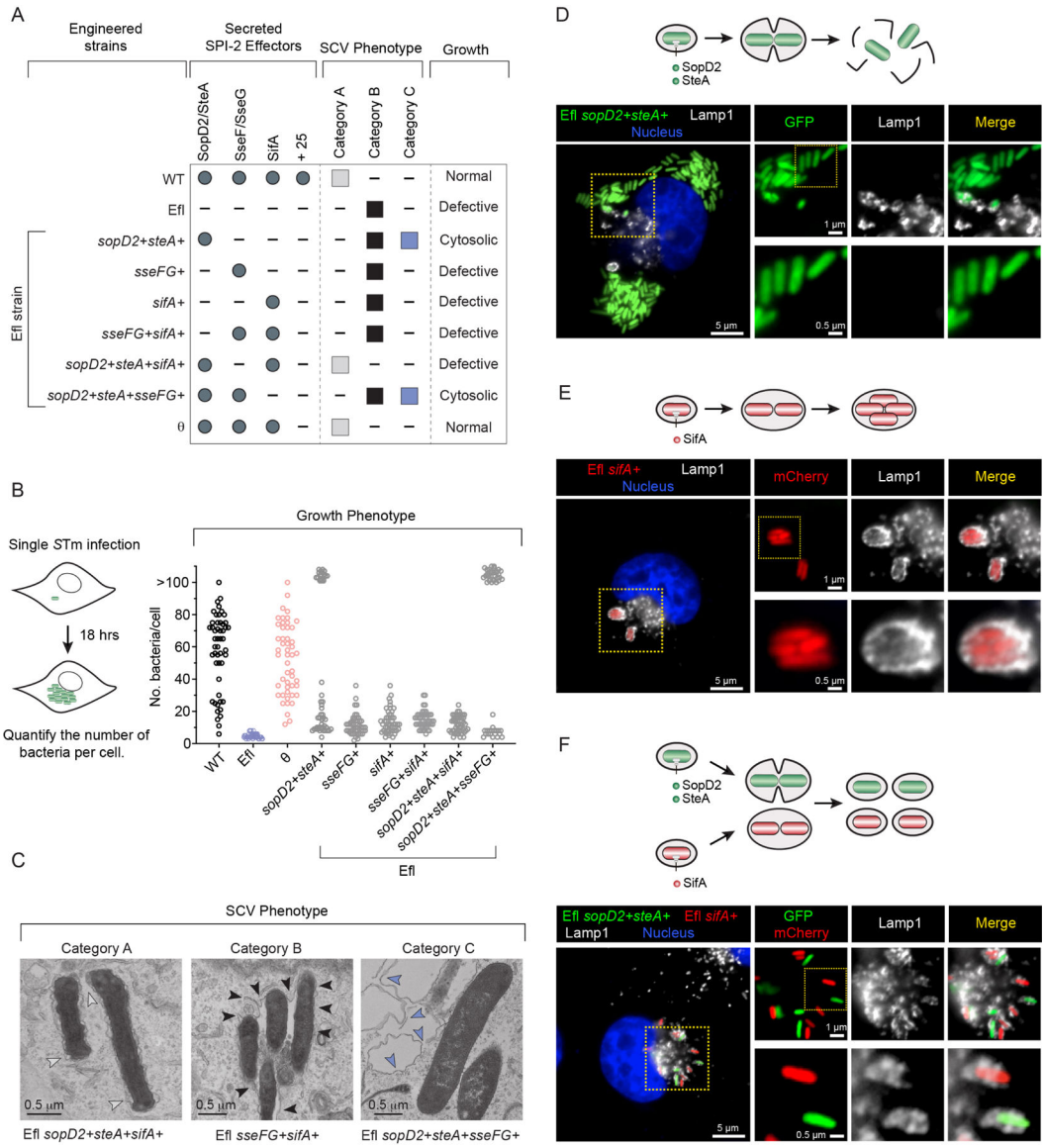

Figure 4 |. Phenotypic profiling of the θ gene network reveals cooperation between essential effector proteins.

(A) Summary of the effector proteins secreted by each strain, the SCV morphological category, and replication phenotype of the indicated engineered *S*Tm Efl strains.

(B) Graph showing the number of individual *S*Tm bacteria within H1299 cells at 18 h p.i.. The number of internalized bacteria per cell was scored by fluorescent microscopy (cartoon). Each dot represents the number of individual bacterial clones in a single infected H1299 cell. 50 infected cells were scored for each strain in two independent experiments.

(C) Representative TEM images of H1299 cells infected with the *S*Tm strains indicated. Category A: individual bacterium was found in an autonomous SCV membrane (white arrowheads). Category B: multiple bacteria were enclosed in one single SCV (black arrowheads). Category C: bacteria disrupted the SCV membranes and replicated in the cell cytosol (blue arrowheads).

(D-F) Cartoon depiction of the SCV morphological progression (top) and representative widefield fluorescence microscopy images (bottom) showing H1299 cells infected with GFP-expressing Efl *sopD2*$^{+}$*steA*$^{+}$ (D), or mCherry-expressing Efl *sifA*$^{+}$ (E), or a 1:1 mixture of both (F) for 18 h. The nucleus (blue) and endogenous Lamp1 (white) are shown. Higher magnification images are shown in the boxed regions.
See also Figure S4.

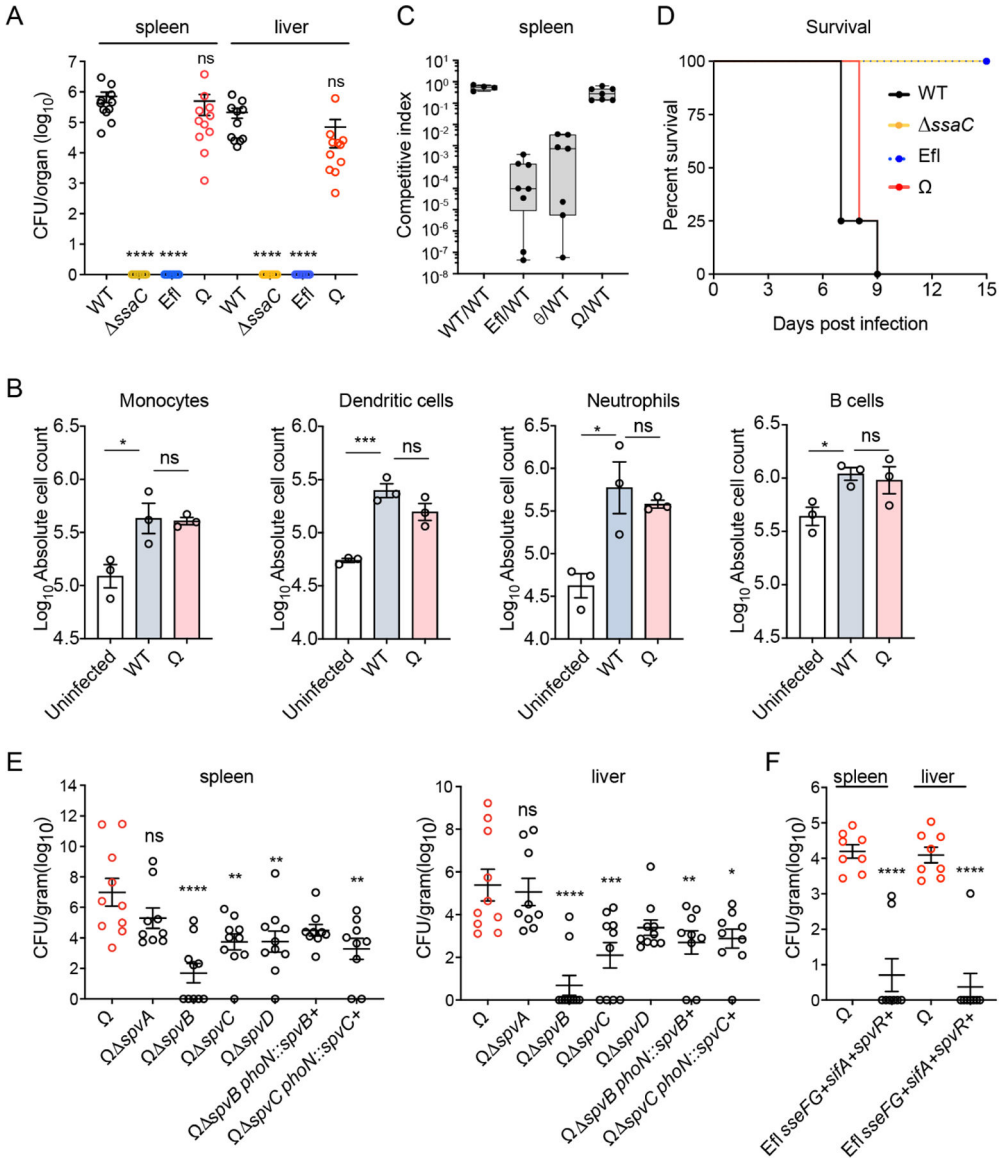

Figure 5 |. *STm* Ω: a minimal effector strain that supports *in vivo* pathogenesis.

(A, E, F) *S*Tm load in spleen and liver of orally infected C57BL/6 mice at 4 days post-infection by the oral route. Data include mice from two independent cohorts. For A and E, Statistical significance in comparison to *S*Tm WT was determined using the one-way ANOVA. For F, Statistical significance was determined using Student's t test. (*, 0.01<p<0.05. **, p<0.01. ***, p<0.001. ****, p<0.0001. ns, p>0.05).

(B) C57BL/6 mice were infected with *S*Tm WT or *S*Tm Ω by the oral route. Immune cell counts from spleen of uninfected mice; *S*Tm WT or *S*Tm Ω infected mice were determined as described in methods. For quantifications, the means ± SEM are shown. Data are representative of three independent experiments. Statistical significance was determined using the one-way ANOVA. (*, 0.01<p<0.05. ***, 0.0001<p<0.001.ns, p>0.05).

(C) Box and Whisker plot of competitive indexes (C.I.) of *S*Tm strains recovered from spleens of C57BL/6 mice 4 days post infection. Mice were inoculated orally with 5×10^8

CFUs of the WT (Δ*phoN*) strain and 5×10^8 CFUs of the comparison strain. C.I. was determined as described in the Methods section. Data include mice from two independent cohorts.

(D) C57BL/6 mice were infected with different *S*Tm strains by the oral route. Survival rate were followed for 15 days. Each group contained 8 mice from two independent cohorts. See also Figure S5.

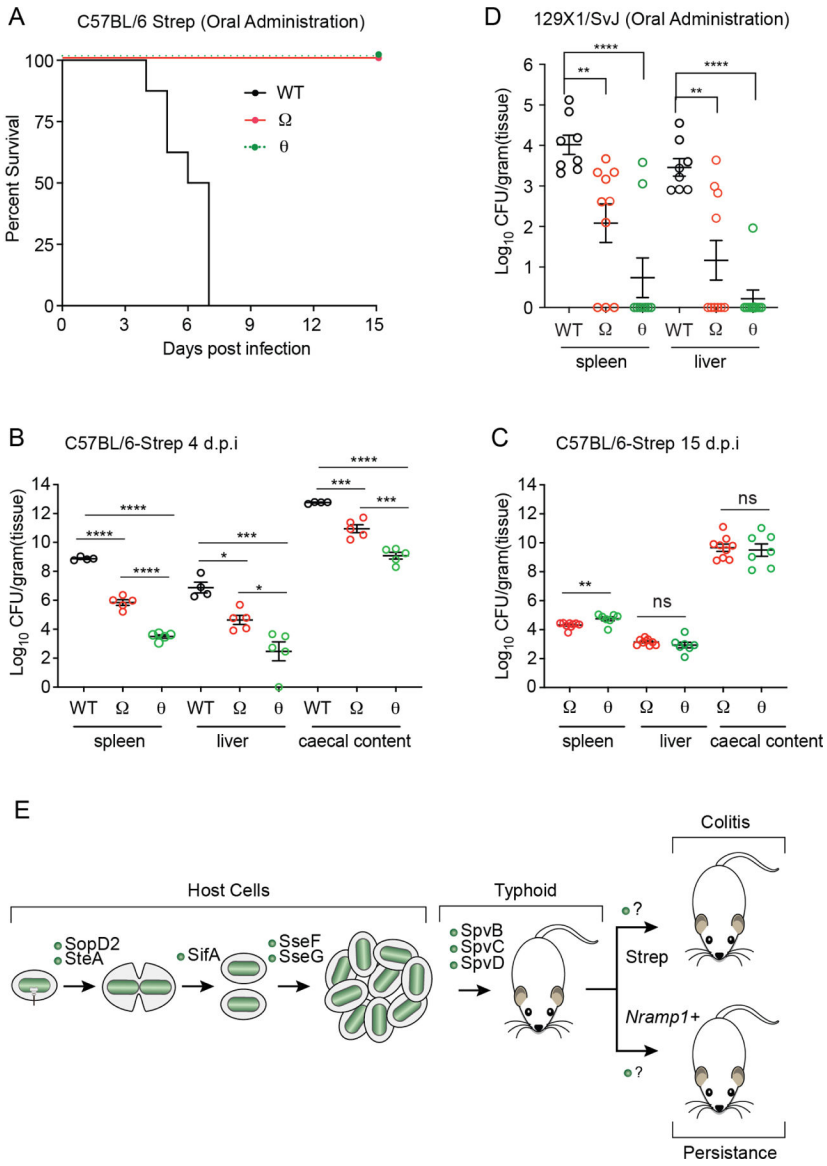

Figure 6 |. *S*Tm adaptation to different environmental conditions.

(A) C57BL/6 mice treated with streptomycin for 24 h were infected by oral gavage with the *S*Tm strain indicated and survival rates were followed for 15 days. Data are from 8 mice per group in two independent cohorts.

(B-C) C57BL/6 mice were treated as in Figure 6A and the bacterial load in spleen, liver, and caecal content of the infected mice were determined at 4 days post-infection (B) and 15 days post-infection (C). Data show individual mice and mean bacterial load from two independent cohorts. Error bars show SEM. Statistical significance was determined using the one-way ANOVA for (B) and Student's t test for (C). (*, 0.01<p<0.05. **, p<0.01. ***, p<0.001. ****, p<0.0001. ns, p>0.05).

(D) 129X1/SvJ mice were infected with the indicated *S*Tm strains by oral gavage. Bacterial load in spleen and liver of the infected mice were determined at 21 days post-infection. Data show individual mice and mean bacterial load from two independent cohorts. Error bars

show SEM. Statistical significance was determined using the one-way ANOVA. (**, p<0.01. ****, p<0.0001).

(E) Cartoon depiction of the role of effector genes in SCV biogenesis and promoting *S*Tm infection pathogenesis in distinct mouse models.

See also Figure S6.

Table 1.

Presence (gene name) or absence (Δ or –) of SPI-2 effector genes in selected STm strains

Order	Single Deletions	*S*Tm Δ5	*S*Tm Δ10	*S*Tm Δ15	Efl (*)	θ (*)	Ω(*)
1	Δ*spvR*						*spvR*
2	Δ*pipAB*						
3	Δ*pipB2*						
4	Δ*gtgA*						
5	Δ*sifB*						
6	Δ*gtgEsteI*	*gtgEsteI*					
7	Δ*steBsseJ*	*steBsseJ*					
8	Δ*pipD*	*pipD*					
9	Δ*sseL*	*sseL*					
10	Δ*gogBsteE*	*gogBsteE*					
11	Δ*sopD2*	*sopD2*	*sopD2*			*sopD2*	*sopD2*
12	Δ*slrP*	*slrP*	*slrP*				
13	Δ*steA*	*steA*	*steA*			*steA*	*steA*
14	Δ*steD*	*steD*	*steD*				
15	Δ*sspH2*	*sspH2*	*sspH2*				
16	Δ*sseK2*	*sseK2*	*sseK2*	*sseK2*			
17	Δ*sseK3*	*sseK3*	*sseK3*	*sseK3*			
18	Δ*steC*	*steC*	*steC*	*steC*			
19	Δ*cigR*	*cigR*	*cigR*	*cigR*			
20	Δ*sseK1*	*sseK1*	*sseK1*	*sseK1*			
21	Δ*srfJ*	*srfJ*	*srfJ*	*srfJ*			
22	Δ*sseFG*	*sseFG*	*sseFG*	*sseFG*		*sseFG*	*sseFG*
23	Δ*sifA*	*sifA*	*sifA*	*sifA*		*sifA*	*sifA*

* The *steD* and *sseK2* genes were deleted together in the strains indicated (see Methods Details).

KEY RESOURCES TABLE

REAGENT or RESOURCE	SOURCE	IDENTIFIER
Antibodies		
anti Lamp1	Abcam	Cat#AB25630
Goat anti-Mouse IgG (H+L) secondary antibody, Rhodamine	Invitrogen	Cat#31660
Goat anti-Mouse IgG (H+L) secondary antibody, Alexa Fluor 647	Invitrogen	Cat#A21235
See Table S4 for the antibodies used in the immunophenotyping	See Table S4	See Table S4
Bacterial and Virus Strains		
E. coli, DH5α λpir, F– endA1 hsdR17 ($r_{-}m^{+}$) supE44 thi-1 recA1 gyrA relA1 Δ(lacZYA-argF)U189 Φ80lacZΔM15 λpir	(Pal et al 2005)	DH5α λpir
Thi thr leu tonA lacY supE recA::RP4-2-Tc::Mu Km λpir	(Simon et al 1983)	SM10 λpir
*S*Tm, SL1344	(Hoiseth & Stocker 1981)	WT
SL1344 Δ*spvR*	This study	NA101
SL1344 Δ*pipAB*	This study	NA102
SL1344 Δ*pipB2*	This study	NA103
SL1344 Δ*gtgA*	This study	NA104
SL1344 Δ*sifB*	This study	NA105
SL1344 Δ*gtgEsteI*	This study	NA106
SL1344 Δ*steBsseJ*	This study	NA107
SL1344 Δ*pipD*	This study	NA108
SL1344 Δ*sseL*	This study	NA109
SL1344 Δ*gogBsteE*	This study	NA110
SL1344 Δ*sopD2*	This study	NA111
SL1344 Δ*slrp*	This study	NA112
SL1344 Δ*steA*	This study	NA113
SL1344 Δ*steD*	This study	NA114
SL1344 Δ*sspH2*	This study	NA115
SL1344 Δ*sseK2*	This study	NA116
SL1344 Δ*sseK3*	This study	NA117
SL1344 Δ*steC*	This study	NA118
SL1344 Δ*cigR*	This study	NA119
SL1344 Δ*sseK1*	This study	NA120
SL1344 Δ*srfJ*	This study	NA121
SL1344 Δ*sseFG*	This study	NA122
SL1344 Δ*sifA*	This study	NA123
SL1344 Δ*steDsseK2*	This study	NA124
SL1344 Δ*ssaC*	This study	NA125
SL1344 Δ*invG*	This study	NA126
SL1344 Δ*sopD2* Δ*steA*	This study	NA127
SL1344 WT (*pBBR1MCS-6y)* (Cm^{R})	This study	NA128

REAGENT or RESOURCE	SOURCE	IDENTIFIER
SL1344 Δ*spvR*::KanR (*pBBR1MCS-6y)* (Cm^R)	This study	NA129
SL1344 Δ*pipAB*::KanR (*pBBR1MCS-6y)* (Cm^R)	This study	NA130
SL1344 Δ*pipB2*::KanR (*pBBR1MCS-6y)* (Cm^R)	This study	NA131
SL1344 Δ*gtgA*::KanR (*pBBR1MCS-6y)* (Cm^R)	This study	NA132
SL1344 Δ*sifB*::KanR (*pBBR1MCS-6y)* (Cm^R)	This study	NA133
SL1344 Δ*gtgEsteI*::KanR (*pBBR1MCS-6y)* (Cm^R)	This study	NA134
SL1344 Δ*steBsseJ*::KanR(*pBBR1MCS-6y)* (Cm^R)	This study	NA135
SL1344 Δ*pipD*::KanR (*pBBR1MCS-6y)* (Cm^R)	This study	NA136
SL1344 Δ*sseL*::KanR *(pBBR1MCS-6y)* (Cm^R)	This study	NA137
SL1344 Δ*gogBsteE*::KanR (*pBBR1MCS-6y)* (Cm^R)	This study	NA138
SL1344 Δ*sopD2*::KanR (*pBBR1MCS-6y)* (Cm^R)	This study	NA139
SL1344 Δ*slrp*::KanR (*pBBR1MCS-6y)* (Cm^R)	This study	NA140
SL1344 Δ*steA*::KanR (*pBBR1MCS-6y)* (Cm^R)	This study	NA141
SL1344 Δ*steD*::KanR (*pBBR1MCS-6y)* (Cm^R)	This study	NA142
SL1344 Δ*sspH2*::KanR (*pBBR1MCS-6y)* (Cm^R)	This study	NA143
SL1344 Δ*sseK2*::KanR (*pBBR1MCS-6y)* (Cm^R)	This study	NA144
SL1344 Δ*sseK3*::KanR (*pBBR1MCS-6y)* (Cm^R)	This study	NA145
SL1344 Δ*steC*::KanR (*pBBR1MCS-6y)* (Cm^R)	This study	NA146
SL1344 Δ*cigR*::KanR (*pBBR1MCS-6y)* (Cm^R)	This study	NA147
SL1344 Δ*sseK1*::KanR (*pBBR1MCS-6y)* (Cm^R)	This study	NA148
SL1344 Δ*srfJ*::KanR (*pBBR1MCS-6y)* (Cm^R)	This study	NA149
SL1344 Δ*sseFG*::KanR (*pBBR1MCS-6y)* (Cm^R)	This study	NA150
SL1344 Δ*sifA*::KanR (*pBBR1MCS-6y)* (Cm^R)	This study	NA151
SL1344 Δ*ssaC* (*pBBR1MCS-6y)* (Cm^R)	This study	NA152
SL1344 Δ*sopD2* (*pBBR1MCS-6y)* (Cm^R)	This study	NA153
SL1344 Δ*steA* (*pBBR1MCS-6y)* (Cm^R)	This study	NA154
SL1344 *S*Tm Δ*sopD2* Δ*steA* (*pBBR1MCS-6y)* (Cm^R)	This study	NA155
SL1344 Δ*spvR* Δ*pipAB* Δ*pipB2* Δ*gtgA* Δ*sifB.* This strain is *S*Tm Δ5.	This study	NA156
SL1344 Δ*spvR* Δ*pipAB* Δ*pipB2* Δ*gtgA* Δ*sifB* Δ*gtgEsseI* Δ*steBsseJ* Δ*pipD* Δ*sseL* Δ*gogBsteE.* This strain is *S*Tm Δ10.	This study	NA157
SL1344 Δ*spvR* Δ*pipAB* Δ*pipB2* Δ*gtgA* Δ*sifB* Δ*gtgEsseI* Δ*steBsseJ* Δ*pipD* Δ*sseL* Δ*gogBsteE* Δ*sopD2.* This strain is *S*Tm Δ11.	This study	NA158
SL1344 Δ*spvR* Δ*pipAB* Δ*pipB2* Δ*gtgA* Δ*sifB* Δ*gtgEsseI* Δ*steBsseJ* Δ*pipD* Δ*sseL* Δ*gogBsteE* Δ*sopD2* Δ*slrp.* This strain is *S*Tm Δ12.	This study	NA159
SL1344 Δ*spvR* Δ*pipAB* Δ*pipB2* Δ*gtgA* Δ*sifB* Δ*gtgEsseI* Δ*steBsseJ* Δ*pipD* Δ*sseL* Δ*gogBsteE* Δ*sopD2* Δ*slrp* Δ*steA.* This strain is *S*Tm Δ13.	This study	NA160
SL1344 Δ*spvR* Δ*pipAB* Δ*pipB2* Δ*gtgA* Δ*sifB* Δ*gtgEsseI* Δ*steBsseJ* Δ*pipD* Δ*sseL* Δ*gogBsteE* Δ*sopD2* Δ*slrp* Δ*steA* Δ*steD.* This strain is *S*Tm Δ14.	This study	NA161
SL1344 Δ*spvR* Δ*pipAB* Δ*pipB2* Δ*gtgA* Δ*sifB* Δ*gtgEsseI* Δ*steBsseJ* Δ*pipD* Δ*sseL* Δ*gogBsteE* Δ*sopD2* Δ*slrp* Δ*steA* Δ*steD* Δ*sspH2.* This strain is *S*Tm Δ15.	This study	NA162
SL1344 *S*Tm Δ5 (*pBBR1MCS-6y)* (Cm^R)	This study	NA163

REAGENT or RESOURCE	SOURCE	IDENTIFIER
SL1344 *S*Tm Δ10 (*pBBR1MCS-6y)* (Cm^R)	This study	NA164
SL1344 *S*Tm Δ15 (*pBBR1MCS-6y)* (Cm^R)	This study	NA165
SL1344 *S*Tm Δ11 (*pBBR1MCS-6y)* (Cm^R)	This study	NA166
SL1344 *S*Tm Δ12 (*pBBR1MCS-6y)* (Cm^R)	This study	NA167
SL1344 *S*Tm Δ13 (*pBBR1MCS-6y)* (Cm^R)	This study	NA168
SL1344 *S*Tm Δ14 (*pBBR1MCS-6y)* (Cm^R)	This study	NA169
SL1344 Δ*spvR* Δ*pipAB* Δ*pipB2* Δ*gtgA* Δ*sifB* Δ*gtgEsseI* Δ*steBsseJ* Δ*pipD* Δ*sseL* Δ*gogBsteE* Δ*sopD2* Δ*slrp* Δ*steA* Δ*steDsseK2* Δ*sspH2* Δ*sseK3* Δ*steC* Δ*cigR* Δ*sseK1* Δ*srfJ* Δ*sseFG* Δ*sifA*. This strain is *S*Tm Efl.	This study	NA170
SL1344 *S*Tm Efl *sopD2*$^+$ *steA*$^+$ *sseFG*$^+$ *sifA*$^+$. This strain is *S*Tm θ.	This study	NA171
SL1344 *S*Tm Efl *sopD2*$^+$ *steA*$^+$ *sseFG*$^+$ *sifA*$^+$ *spvR*$^+$. This strain is *S*Tm Ω.	This study	NA172
SL1344 *S*Tm Δ13 *sopD2*$^+$ *steA*$^+$	This study	NA173
SL1344 *S*Tm Efl *sopD2*$^+$ *steA*$^+$	This study	NA174
SL1344 *S*Tm Δ13 *sopD2*$^+$ *steA*$^+$ (*pBBR1MCS-6y)* (Cm^R)	This study	NA175
SL1344 *S*Tm Efl *sopD2*$^+$ *steA*$^+$ (*pBBR1MCS-6y)* (Cm^R)	This study	NA176
SL1344 *S*Tm Efl (*pBBR1MCS-6y)* (Cm^R)	This study	NA177
SL1344 *S*Tm θ (*pBBR1MCS-6y)* (Cm^R)	This study	NA178
SL1344 *S*Tm Efl *sseFG*$^+$	This study	NA179
SL1344 *S*Tm Efl *sifA*$^+$	This study	NA180
SL1344 *S*Tm Efl *sseFG*$^+$ *sifA*$^+$	This study	NA181
SL1344 *S*Tm Efl *sopD2*$^+$ *steA*$^+$ *sifA*$^+$	This study	NA182
SL1344 *S*Tm Efl *sopD2*$^+$ *steA*$^+$ *sseFG*$^+$	This study	NA183
SL1344 *S*Tm Efl *spvR*$^+$	This study	NA184
SL1344 *S*Tm Efl *sseFG*$^+$ (*pBBR1MCS-6y)* (Cm^R)	This study	NA185
SL1344 *S*Tm Efl *sifA*$^+$ (*pBBR1MCS-6y)* (Cm^R)	This study	NA186
SL1344 *S*Tm Efl *sseFG*$^+$ *sifA*$^+$ (*pBBR1MCS-6y)* (Cm^R)	This study	NA187
SL1344 *S*Tm Efl *sopD2*$^+$ *steA*$^+$ *sifA*$^+$ (*pBBR1MCS-6y)* (Cm^R)	This study	NA188
SL1344 *S*Tm Efl *sopD2*$^+$ *steA*$^+$ *sseFG*$^+$ (*pBBR1MCS-6y)* (Cm^R)	This study	NA189
SL1344 *S*Tm Efl *sifA*$^+$ (*pDP151)* (Amp^R)	This study	NA190
SL1344 *S*Tm Efl *sopD2*$^+$ *steA*$^+$ (*pDP151)* (Amp^R)	This study	NA191
SL1344 *S*Tm θ (*pDP151)* (Amp^R)	This study	NA192
SL1344 *S*Tm Efl *sseFG*$^+$ (*pDP151)* (Amp^R)	This study	NA193
SL1344 *S*Tm Efl *sseFG*$^+$ *sifA*$^+$ *spvR*$^+$	This study	NA194
SL1344 *phoN*::Cm^R	(Winter et al 2014)	SW759
SL1344 *S*Tm Ω Δ*spvA*	This study	NA195
SL1344 *S*Tm Ω Δ*spvB*	This study	NA196
SL1344 *S*Tm Ω Δ*spvC*	This study	NA197
SL1344 *S*Tm Ω Δ*spvD*	This study	NA198

REAGENT or RESOURCE	SOURCE	IDENTIFIER
SL1344 *S*Tm Ω Δ*spvB phoN::spvB*	This study	NA199
SL1344 *S*Tm Ω Δ*spvC phoN::spvC*	This study	NA200
Chemicals, Peptides, and Recombinant Proteins		
5-Bromo-4-chloro-3-indolyl phosphate (X-phos)	Chem-Impex	Cat#20915
Agar	Becton Dickinson	Cat#214010
Ampicillin sodium salt	Millipore Sigma	Cat#A9518
Brain Heart Infusion broth	Becton Dickinson	Cat#237500
Bovine Serum Albumin (BSA)	Fisher Scientific	Cat#BP1605
Carbenicillin, disodium salt	VWR	Cat#J358
Chloramphenicol	Alfa Aesar	Cat#B20841
DMEM-High Glucose	Millipore Sigma	Cat#D6429
DMEM/F12	Millipore Sigma	Cat#D8437
Fetal Bovine Serum (FBS)	Sigma	Cat#F4135
Formaldehyde solution	Fisher Scientific	Cat#F79
Gentamicin	Quality Biological	Cat#120-098-661
Gibson Assembly Master Mix	NEB	Cat#E2611L
Glucose	Fisher Chemical	Cat#D14-212
Kanamycin sulfate	Millipore Sigma	Cat#K1377
LB broth	Fisher Scientific	Cat#BP9722
LB agar	Fisher Scientific	Cat#BP9724
Nutrient Broth	Becton Dickinson	Cat#234000
Paraformaldehyde (4%)	Alfa Aesar	Cat#47392
PBS	Sigma	Cat#D8537
RPMI Medium 1640	Thermo Fisher	Cat#11875
Saponin	MP Biomedicals	Cat#102855
Sodium Chloride	Fisher Scientific	Cat#BP358
Streptomycin sulfate	Fisher Scientific	Cat#BP910
Sucrose	Fisher Science Education	Cat#S25590
Triton X-100	Fisher Scientific	Cat#BP151
Tryptone	Becton Dickinson	Cat#211705
Yeast Extract	Becton Dickinson	Cat#212750
Experimental Models: Cell Lines		
Hela	Hela	Hela
RAW264.7	RAW264.7	RAW264.7
HCT116	HCT116	HCT116
T84	T84	T84
H1299	H1299	H1299
Experimental Models: Organisms/Strains		
C57BL/6J mice	Jackson Lab	000664

REAGENT or RESOURCE	SOURCE	IDENTIFIER
129X1/SvJ mice	Jackson Lab	000691
C57BL/6J *Nramp1*^{G169} mice	(Arpaia et al 2011)	N/A
Oligonucleotides		
See Table S1–S3 for full list of primers used in this study	This Study	See Table S1–S3
Recombinant DNA		
GFP expression plasmid	(Murphy et al 2002)	*pBBR1MCS-6y*
mCherry expression plasmid	(Burnaevskiy et al 2013)	pDP151
ori(R6K) *mobRP4* Cm^r Tet^r *sacRB*	(Kingsley et al 1999)	pRDH10
Template plasmid for FRT-flanked Kan^R cassette	(Datsenko & Wanner 2000)	pKD4
Red recombinase expression plasmid	(Datsenko & Wanner 2000)	pKD46
Helper plasmid to eliminate the Kan^R cassette	(Datsenko & Wanner 2000)	pCP20
downstream region of *S*Tm *spvR* in pRDH10	This Study	pNA101
downstream region of *S*Tm *pipAB* in pRDH10	This Study	pNA102
downstream region of *S*Tm *pipB2* in pRDH10	This Study	pNA103
downstream region of *S*Tm *gtgA* in pRDH10	This Study	pNA104
downstream region of *S*Tm *sifB* in pRDH10	This Study	pNA105
downstream region of *S*Tm *gtgEsseI* in pRDH10	This Study	pNA106
downstream region of *S*Tm *steBsseJ* in pRDH10	This Study	pNA107
downstream region of *S*Tm *pipD* in pRDH10	This Study	pNA108
downstream region of *S*Tm *sseL* in pRDH10	This Study	pNA109
downstream region of *S*Tm *gogBsteE* in pRDH10	This Study	pNA110
downstream region of *S*Tm *sopD2* in pRDH10	This Study	pNA111
downstream region of *S*Tm *slrp* in pRDH10	This Study	pNA112
downstream region of *S*Tm *steA* in pRDH10	This Study	pNA113
downstream region of *S*Tm *steD* in pRDH10	This Study	pNA114
downstream region of *S*Tm *sspH2* in pRDH10	This Study	pNA115
downstream region of *S*Tm *sseK2* in pRDH10	This Study	pNA116
downstream region of *S*Tm *sseK3* in pRDH10	This Study	pNA117
downstream region of *S*Tm *steC* in pRDH10	This Study	pNA118
downstream region of *S*Tm *cigR* in pRDH10	This Study	pNA119
downstream region of *S*Tm *sseK1* in pRDH10	This Study	pNA120
downstream region of *S*Tm *srfJ* in pRDH10	This Study	pNA121
downstream region of *S*Tm *sseFG* in pRDH10	This Study	pNA122
downstream region of *S*Tm *sifA* in pRDH10	This Study	pNA123
downstream region of *S*Tm *steDsseK2* in pRDH10	This Study	pNA124
upstream and downstream regions of *S*Tm *spvA* in pRDH10	This Study	pNA125

REAGENT or RESOURCE	SOURCE	IDENTIFIER
upstream and downstream regions of *S*Tm *spvB* in pRDH10	This Study	pNA126
upstream and downstream regions of *S*Tm *spvC* in pRDH10	This Study	pNA127
upstream and downstream regions of *S*Tm *spvD* in pRDH10	This Study	pNA128
Fragment of *phoN* cloned into pGP704	(Spiga et al 2017)	pSW327
Promoter and coding regions of *S*Tm *spvB* in pSW327	This Study	pNA129
Promoter and coding regions of *S*Tm *spvC* in pSW327	This Study	pNA130
Software and Algorithms		
CellCapTure	Stratedigm	https://stratedigm.com/cellcapture/
GraphPad Prism 8	GraphPad Software	https://www.graphpad.com/
FLowJo	BD biosciences	https://www.flowjo.com/
Adobe Illustrator Creative Cloud	Adobe	https://www.adobe.com
Adobe Photoshop Creative Cloud	Adobe	https://www.adobe.com